Review

Not peer-reviewed version

Artificial Intelligence for Mineral Exploration: Methods, Foundation Models, and Future Directions

Ashkan Taghipour *, Richard Scott, Morteza Ghahremani, Mark Jessell, Farid Boussaid, Hamid Laga, Mohammed Bennamoun

Posted Date: 31 July 2026

doi: 10.20944/preprints202607.2303.v1

Keywords: machine learning; mineral exploration; prospectivity mapping; foundation models; deep learning; remote sensing; geochemistry; geophysics; NLP; AI

Article

Artificial Intelligence for Mineral Exploration: Methods, Foundation Models, and Future Directions

Ashkan Taghipour [1,*], Richard Scott [2], Morteza Ghahremani [3], Mark Jessell [4], Farid Boussaid [5], Hamid Laga [6] and Mohammed Bennamoun [1]

[1] The University of Western Australia, Department of Computer Science and Software Engineering, Perth, Western Australia, Australia
[2] Independent Researcher, Australia
[3] Technical University of Munich (TUM), Munich Center for Machine Learning (MCML), Germany
[4] The University of Western Australia, Centre for Exploration Targeting, School of Earth and Oceans, Perth, Western Australia, Australia
[5] The University of Western Australia, Department of Electrical, Electronics and Computer Engineering, Perth, Western Australia, Australia
[6] Murdoch University, School of Information Technology, Perth, Western Australia, Australia
* Correspondence: ashkan.taghipour@research.uwa.edu.au

Abstract

As global demand for minerals in general, and critical minerals in particular, intensifies, discovering new deposits has become a pressing scientific challenge. This task requires integrating heterogeneous geoscientific data, including geophysical, geochemical, remote sensing, geological, and textual sources, across vast underexplored terrains. Such integration poses distinct challenges for Machine Learning (ML), including extreme label scarcity in a natural Positive-Unlabeled setting, spatial non-stationarity that violates independent and identically distributed (i.i.d.) assumptions, and multi-format data heterogeneity. Despite this growing body of work, a unified review connecting classical ML, deep learning, and foundation models across the full exploration pipeline is lacking. This survey reviews ML and foundation models across the mineral exploration pipeline. We cover domain-specific ML for geological, geophysical, geochemical, and remote sensing tasks; mineral prospectivity mapping (MPM) from classical methods through deep learning and 3D prediction; foundation models and NLP-based knowledge extraction across multiple geoscience modalities; and the supporting ecosystem of open datasets, portals, and software. For each area, we assess the current maturity of foundation model applications, identify domain-specific adaptations required, and highlight open gaps where AI research could have significant impact, particularly multi-modal foundation models, cross-region transfer learning, uncertainty-aware prediction, and AI agents for exploration decision support. A curated list of resources is available on the project page.

Keywords: machine learning; mineral exploration; prospectivity mapping; foundation models; deep learning; remote sensing; geochemistry; geophysics; NLP; AI

---

1. Introduction

The growing global demand for minerals and mining resources, driven by the clean energy transition, battery technology, and advancing electronics, has made the discovery of new mineral deposits increasingly important [1]. Mineral exploration is the process of finding and evaluating these deposits. This process generates multi-modal data spanning four main types: **(a)** gridded geophysical surveys (gravity, magnetics, electromagnetics) measuring subsurface physical properties, **(b)** multi-element geochemical samples capturing rock and soil composition, **(c)** multi- and hyperspectral satellite imagery revealing surface mineralogy, and **(d)** categorical geological maps describing rock types and structures [2,3]. Interpreting these datasets has traditionally relied on domain experts, a process that is time-consuming, subjective, and difficult to scale [4]. Artificial Intelligence (AI) and

 doi:10.20944/preprints202607.2303.v1

Machine Learning (ML) offer the potential to integrate these heterogeneous sources, identify subtle patterns across modalities, and accelerate deposit discovery [5].

Despite this potential, applying AI to mineral exploration is not straightforward. One of the main challenges is the extreme scarcity of labeled data. Known mineral deposits are rare relative to the vast areas that must be evaluated. For example, across an entire geological region there may be only a few dozen known deposits of a given commodity, while most of the area has never been systematically explored. Critically, the absence of a known deposit does not mean the area is barren; it simply means it has not been tested. Unlike standard binary classification, where negative labels are reliable, the "negative" class in mineral exploration is fundamentally unlabeled. This makes the problem a natural instance of Positive-Unlabeled (PU) learning [6], where models are trained from confirmed positives and unlabeled examples rather than from confirmed positives and reliable negatives. This setting is also related to Multi-Instance Learning (MIL), where supervision is provided at the bag level rather than for individual instances, analogous to knowing that a region contains mineralization without knowing the precise locations within it.

A second challenge is that geoscience data is inherently spatial, and standard ML assumptions do not hold. Nearby locations tend to have similar geological properties. For example, if a soil sample at one location shows elevated copper concentration, samples collected a few hundred meters away are likely to show similar enrichment because they overlie the same geological unit. This spatial dependence violates the independence assumption that most models rely on [7]. This spatial autocorrelation means that naive random train-test splits produce overly optimistic results, as test samples may be correlated with nearby training samples [8]. More fundamentally, the geological processes that control mineral deposit formation vary across regions. A model trained in one geological setting may not generalize to another because the same input features can have different meanings in different geological contexts [9]. This non-stationarity makes transfer learning across regions a particularly difficult open problem.

A third challenge is the heterogeneity of geoscience data itself. A single study may need to combine gridded geophysical surveys at 50-meter resolution with geochemical samples collected at irregular intervals of several kilometers, alongside categorical geological maps and multi-band satellite imagery [2,3]. These data come from different organizations, and collected at different times, using different instruments and standards, resulting in inconsistencies in format, quality, and coverage [10]. When exploration targets lie beneath cover, surface signatures are absent entirely, and prediction must rely on indirect geophysical and geochemical measurements [2]. Integrating these heterogeneous, incomplete, and indirect data sources into a coherent predictive framework remains a fundamental challenge.

Considering these challenges, AI methods have been developed for mineral exploration. Within individual geoscience domains, ML has improved how each data type is processed and interpreted: automated lithological mapping from geological and remote sensing data [11,12], physics-constrained inversion of geophysical surveys [13,14], spatially aware geochemical anomaly detection [15], and mineral signature extraction from hyperspectral imagery [16,17]. These domain-specific outputs are then integrated through Mineral Prospectivity Mapping (MPM), the task of predicting which areas are most likely to host mineral deposits [4]. MPM is the most established AI application in mineral exploration, with methods spanning classical approaches such as Weights of Evidence [18] and Random Forests [19], deep learning architectures [20–22], and more recent directions including transfer learning across geological regions [23] and 3D prospectivity prediction at depth [24].

Foundation models, large-scale models pre-trained on broad datasets and adapted to downstream tasks [25], have emerged across multiple geoscience modalities. Earth observation models learn general-purpose representations from satellite imagery [26,27], geophysical models target subsurface understanding [28,29], and geoscience Large Language Models (LLMs) can reason about geological concepts [30–32]. Complementary Natural Language Processing (NLP) tools, including domain-specific word embeddings [33], named entity recognition [34], and knowledge graphs [35], convert the

 doi:10.20944/preprints202607.2303.v1

knowledge in geological text into structured, machine-readable inputs [36]. These approaches reduce the dependence on large labeled datasets and open new possibilities for knowledge transfer across tasks and regions.

Supporting this research is a growing ecosystem of open datasets, data portals, and software tools. Purpose-built training datasets such as the Noddyverse [37] provide synthetic geological models for supervised learning. National geological surveys in Australia [38], Canada [39], and the United States [40] maintain open data portals with geophysical, geochemical, and geological coverage. Open-source frameworks such as UNCOVER-ML [41], TorchGeo [42], and SimPEG [43] provide, respectively, end-to-end pipelines for prospectivity mapping, remote sensing deep learning, and geophysical inversion. This ecosystem is critical for enabling reproducibility and lowering the barrier to entry for AI researchers.

This survey provides a structured review of AI, including foundation models, for mineral exploration. We cover the exploration pipeline, i.e., the process of finding and evaluating deposits before mining begins, including domain-specific methods, prospectivity mapping, foundation models, NLP, and the supporting data ecosystem. We do not cover mining operations such as ore processing, grade control, or mine planning.

Several recent reviews have addressed parts of this landscape. Bergen et al. [44] reviewed ML for data-driven discovery in solid Earth geoscience broadly, covering seismology, remote sensing, and subsurface characterization. Zuo et al. [45] focused on deep learning for geochemical mapping, while Dramsch [46] provided a historical perspective spanning 70 years of ML in geoscience. Zuo [47] introduced geodata science for MPM, and Zuo et al. [48] systematically addressed uncertainties in GIS-based prospectivity mapping. Sun et al. [49] reviewed deep learning architectures for MPM, focusing on network design choices and training strategies for prospectivity prediction. Yang et al. [50] provided a broader treatment of AI for mineral exploration from a data science perspective, covering data integration, feature engineering, and modeling workflows. Fu et al. [51] traced the evolution of ML-based prospectivity prediction over the period 2016–2025. Zhang et al. [52] surveyed foundation models for geoscience, covering key techniques and advances but without connecting them to the mineral exploration pipeline. Table 1 provides a systematic comparison of these surveys across key dimensions.

Table 1. Comparison of related surveys across key dimensions of the mineral exploration AI pipeline. Domain ML refers to ML methods applied within individual geoscience modalities (geological mapping, geophysics, geochemistry, and remote sensing) that produce evidence layers for downstream integration.

Survey	Year	MPM	Domain ML	FMs	NLP/LLM	Uncertainty	3D	Data Ecosystem
Bergen et al. [44]	2019	No	Yes	No	No	No	No	No
Zuo et al. [45]	2019	Yes	Yes	No	No	No	No	No
Dramsch [46]	2020	Yes	Yes	No	No	No	No	No
Zuo [47]	2020	Yes	No	No	No	Yes	No	No
Zuo et al. [48]	2021	Yes	No	No	No	Yes	No	No
Sun et al. [49]	2024	Yes	No	No	No	Yes	No	No
Yang et al. [50]	2024	Yes	Yes	No	No	No	No	No
Zhang et al. [52]	2024	No	No	Yes	Yes	No	No	No
Fu et al. [51]	2025	Yes	No	No	No	No	No	No
Ours	**2026**	**Yes**	**Yes**	**Yes**	**Yes**	**Yes**	**Yes**	**Yes**

Our survey complements these works in three respects. **First**, whereas prior surveys treat foundation models within a single modality or omit them entirely, we assess foundation models across four geoscience modalities (Earth observation, geophysics, language, and vision–language) within a single comparative framework (Table 4). We classify each model by its maturity for mineral exploration: demonstrated in an exploration context, architecturally ready but untested, or addressing a capability that remains open (Section 5). This cross-modal view reveals where building blocks already exist and where critical gaps remain, particularly the absence of foundation models for gravity, magnetic, and electromagnetic data. **Second**, we trace a complete pathway from unstructured geological text to quantitative prospectivity prediction, connecting NLP tools (word embeddings, named entity

 doi:10.20944/preprints202607.2303.v1

recognition, knowledge graphs) with the MPM pipeline and showing how text-derived features complement traditional numerical evidence layers (Section 5.3). **Third**, we frame the presentation for an AI/ML audience: geoscience concepts are explained in ML terms, and we highlight the architectural and methodological gaps where AI research could have the greatest impact.

The remainder of this paper is organized as follows. Section 2 provides background on the mineral exploration pipeline, geoscience data modalities, and ML paradigms relevant to this survey. Section 3 reviews ML methods within individual geoscience domains (geological mapping, geophysics, geochemistry, and remote sensing) that produce processed data products, referred to as evidence layers, used as inputs for exploration models. Section 4 covers MPM, which integrates these evidence layers to identify areas favorable for mineral deposit formation. While the methods in Sections 3–4 rely on task-specific supervised learning, recent foundation models offer pre-trained representations that can reduce label dependence across the pipeline. Section 5 presents foundation models and NLP-based knowledge extraction across geoscience modalities, identifying where these emerging tools have and have not been applied to mineral exploration. Section 6 describes the supporting ecosystem of datasets, data portals, frameworks, and tools. Section 7 consolidates open challenges and research opportunities, organized by maturity: issues addressable with current tools, near-term opportunities requiring domain adaptation, and long-term research frontiers. Section 8 concludes the paper.

2. Background

This section establishes the context for the survey by introducing the mineral exploration pipeline, the principal geoscience data modalities, and the ML paradigms that underpin the methods reviewed in subsequent sections.

2.1. The Mineral Exploration Pipeline

Mineral exploration proceeds through a series of stages, progressively narrowing the search area [2,4] (Figure 1). At the broadest scale, *area selection* identifies regions worth investigating based on geological characteristics such as rock types, structural features, and the known distribution of mineral deposits [2]. *Target generation* narrows the search further by combining geological maps, geophysical surveys, geochemical sampling, and remote sensing imagery to pinpoint specific areas of interest [4,53]. *Target testing* involves detailed field work, drilling, and estimating the size and grade of any deposit found [2,3]. ML methods are increasingly applied across all stages, but are most prominent in area selection and target generation, where data integration and pattern recognition are central tasks.

 doi:10.20944/preprints202607.2303.v1

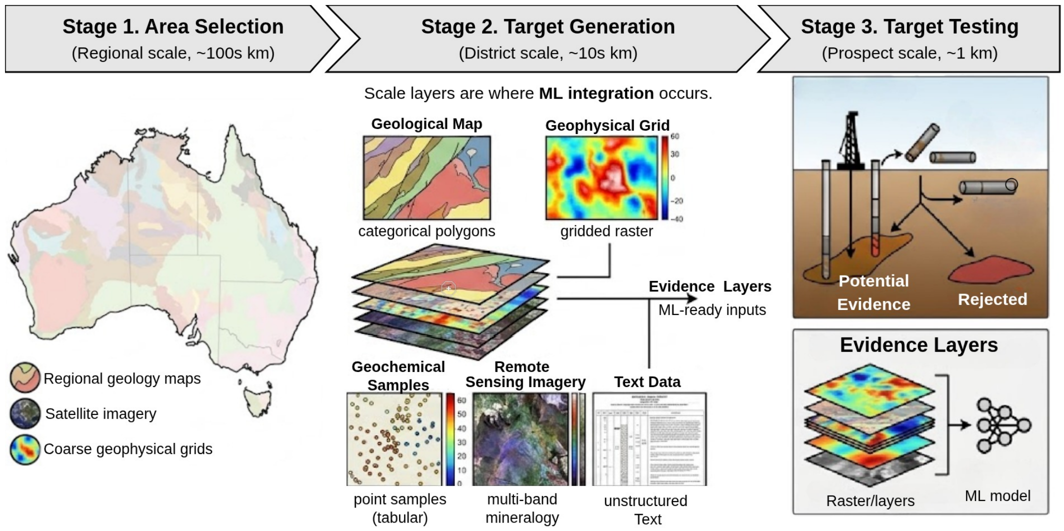

Figure 1. Mineral Exploration Pipeline and Data Modalities. An overview of the exploration workflow demonstrating the spatial scales and data types utilized at each stage. Stage 1 (Area Selection) uses regional-scale (∼100s km) geology, satellite imagery, and coarse geophysics to identify broad regions of interest. Stage 2 (Target Generation) operates at the district scale (∼10s km) and relies heavily on data integration; raw heterogeneous data, including geological maps (categorical polygons), geophysical surveys (gridded rasters), geochemical assays (tabular point samples), remote sensing (multi-band imagery), and unstructured text—are processed into stacked 'evidence layers' that serve as inputs for machine learning models. Stage 3 (Target Testing) involves prospect-scale (∼1 km) physical validation, such as drill core sampling, to confirm or reject predicted deposits.

2.2. Geoscience Data Modalities

The multi-disciplinary nature of mineral exploration gives rise to diverse data modalities (Figure 1), each with distinct characteristics relevant to ML:

- **Geological data:** Geological data comprise maps, drillhole logs, structural measurements, lithological and stratigraphic classifications, and tectonic data such as fault networks and plate reconstruction models [54,55]. Geological map data comprise three geometrically distinct feature types requiring different ML representations: polygonal regions describing lithology (categorical), point measurements of structural orientations such as bedding and foliation (continuous angular quantities), and polyline features such as fault traces and fold axes that control fluid flow and mineral deposition [4]. These include both spatial (vector and raster) and tabular formats.
- **Geophysical data:** Geophysical data consist of gridded surveys of gravity, magnetics, radiometrics, electromagnetics, and seismic measurements [3]. These are typically raster datasets with varying resolutions. Different methods sense different depth ranges, from near-surface (ground-penetrating radar, metres) to crustal scale (magnetotellurics, tens of kilometres) [3], so fusing or comparing geophysical images without accounting for their depth sensitivity can be misleading.
- **Geochemical data:** Geochemical data include stream sediment, soil, rock chip, and drill core assay results providing multi-element chemical compositions [56,57]. These are typically point-sampled tabular data (sample locations with multi-element assay values), inherently compositional (concentrations sum to a constant) [58], and spatially irregular.
- **Remote sensing data:** Remote sensing data include multi-spectral and hyperspectral satellite imagery, as well as high-resolution aerial photography and LiDAR [59]. The optical sources provide multi-band raster imagery (or hyperspectral data cubes) with continuous spatial coverage and rich spectral information, while LiDAR captures 3D surface geometry.
- **Textual data:** Textual data comprise geological reports, exploration company announcements, scientific publications, and government survey records containing domain knowledge in unstructured text and tabular formats [36,60,61].

doi:10.20944/preprints202607.2303.v1

Table 2 summarizes how the native format and spatial sampling of each modality constrain the choice of ML representation and modeling approach.

Table 2. Geoscience data modalities and their implications for ML representation and modeling choices.

Data Modality	Native Format	Spatial Sampling	Representation for ML	Common Approach	Key Constraint
Geological maps	Vector (polygons, polylines, points)	Irregular boundaries	Rasterization with one-hot encoding; or graph from topology	RF/XGBoost on encoded cell features	Categorical; spatial topology lost in rasterization
Geophysical surveys	Regular grids	50m–1km (airborne); coarser for satellite	Derivative features (gradients, upward continuation); or direct grid input	RF/XGBoost on derived features	Different methods sense different depths; non-unique inversion
Geochemical assays	Irregular point samples (tabular)	50m–5km (varies by survey type)	Log-ratio transform (CLR/ILR); interpolation to grid; or spatial graph	RF/XGBoost on per-sample features; autoencoders for anomaly detection	Compositional data (concentrations sum to constant); irregular spacing
Remote sensing	Multi-band raster (4–400 bands)	Regular (0.3–90m per pixel)	Band ratios and indices; or direct image input	CNN/ViT on image patches	Surface only; spectral vs. spatial resolution trade-off
Textual data	Unstructured documents	Spatially grounded via metadata	Embeddings, named entity recognition, knowledge graphs	Word2vec/BERT for feature extraction; LLM for reasoning	Domain-specific vocabulary; requires spatial linking to map units

In practice, these raw data are processed into input features for ML models. In mineral exploration, these processed features are called *evidence layers* [4,53]. Evidence layers can take different forms depending on the data source: raster grids (e.g., a gravity anomaly map from geophysical surveys), point-sampled tabular data (e.g., geochemical assay results at sample locations), or categorical maps (e.g., lithological classifications from geological mapping) [3,59]. Each layer captures one aspect of the geological environment relevant to deposit formation. Constructing these evidence layers from raw data is itself a significant ML task (reviewed in Section 3), and their integration for deposit prediction is the focus of MPM (Section 4). A cross-cutting dimension not captured by any single modality is geological time. Relative timing (stratigraphic ordering, cross-cutting relationships) and absolute ages (radiometric dating) constrain which events are relevant to mineralization [2], yet temporal relationships are rarely encoded in current ML workflows.

3. ML Across Geoscience Domains

ML has been applied within each of the four geoscience domains: geology, geophysics, geochemistry, and remote sensing [5]. These ML methods improve how each data type is processed and interpreted, producing higher-quality evidence layers that feed into MPM (Section 4). This section reviews ML applications within each of these four domains.

 doi:10.20944/preprints202607.2303.v1

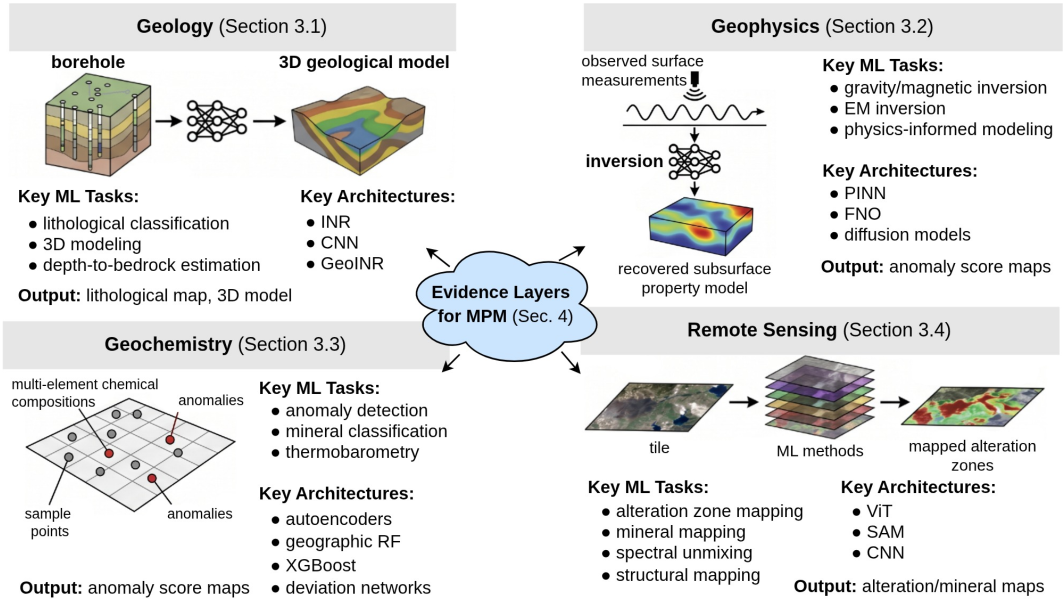

Figure 2. A visual summary of the key ML methods, tasks, architectures, and resulting data products across the four geoscience domains: geology, geophysics, geochemistry, and remote sensing.

3.1. Geological Mapping and 3D Modeling

3.1.1. Lithological Mapping and Classification

Lithological mapping is the task of identifying and spatially classifying rock types across a region. It provides a key evidence layer for mineral exploration because different deposit types are associated with specific host rocks. The main ML challenge is that ground truth labels typically come from sparse field observations or limited drillhole data, while the goal is to produce continuous spatial predictions across large areas.

Early ML approaches treated this as pixel-wise classification, assigning a rock type to each location without considering spatial context. Spatially constrained Bayesian networks [11] improved on this by incorporating geological prior knowledge and spatial context into the classification. Contrastive graph attention networks [12] extended the approach further by fusing multiple data sources through a graph structure that captures spatial relationships between locations. When labeled geological data are scarce, transfer learning from natural image domains has proven effective. For example, Convolutional Neural Networks (CNNs), pre-trained on natural images, have been fine-tuned for carbonate rock classification with small training sets [62]. PetroMind [63] combines rock image classification with textual description generation for petrographic analysis. CNNs have also been applied to photographs of drill core samples for automated lithological logging [64].

3.1.2. 3D Geological Modeling with Deep Learning

Understanding the 3D structure of the subsurface is fundamental to mineral exploration, but direct observations are limited to sparse boreholes and surface outcrops. The ML challenge is to interpolate between these sparse observations to build a complete 3D model. GeoINR [65] applied Implicit Neural Representations (INRs) to this task, learning a continuous function that maps 3D spatial coordinates to implicit scalar field values from which geological units are subsequently derived. This approach naturally handles complex geological structures, including faults and discontinuities, and has been extended with Hamiltonian Monte Carlo sampling for uncertainty quantification [66]. At the regional scale, Sub3DNet [67] demonstrated that neural networks can learn spatial relationships from surface observations (geological maps, remote sensing, digital elevation models) and geophysical constraints for subsurface structure mapping. Ghyselincks et al. [68] used generative flow matching [69] to reconstruct 3D geology from surface maps and sparse borehole data, producing multiple probable geological scenarios that can support geophysical inversion and probabilistic modeling. A related

Preprints.org (www.preprints.org) | NOT PEER-REVIEWED | Posted: 31 July 2026 doi:10.20944/preprints202607.2303.v1

task is estimating the depth to bedrock, i.e., the thickness of unconsolidated cover overlying bedrock. This is important for mineral exploration because it determines whether deposits are accessible and how geophysical signals are attenuated. Spatially-enabled ML approaches [70] have shown that incorporating spatial features significantly improves prediction accuracy over standard non-spatial models.

3.2. Geophysical Data Analysis and Inversion

Geophysical surveys measure physical properties of the Earth (such as density, magnetism, electrical conductivity, and seismic velocity) from the earth surface or airborne platforms [3]. The central computational task is *inversion*, i.e., recovering a model of subsurface properties from surface observations. This is a classic inverse problem, typically ill-posed and computationally expensive when solved with traditional numerical methods. ML offers two strategies: learning the inverse mapping directly from simulated data, or embedding physical equations into the network to constrain the solution space.

3.2.1. Gravity and Magnetic Data Analysis

Gravity and magnetic surveys are among the most common geophysical datasets in mineral exploration because they are relatively inexpensive to acquire over large areas [3]. Gravity data reflect density variations in the subsurface, while magnetic data reflect the distribution of magnetic minerals. The ML task is to invert these 2D surface measurements into 3D subsurface models.

CNNs have been trained on synthetic examples to recover 3D subsurface structure from gravity data [71], learning the inverse mapping from observed surface measurements to depth models. Guo et al. [72] take a similar approach for magnetic data, training on synthetic 3D geological models generated using PyNoddy [37]. Adapted-SRGAN [73] addresses a different task: applying super-resolution Generative Adversarial Networks (GANs) to enhance the spatial resolution of airborne magnetic survey maps.

3.2.2. Electromagnetic Methods

Electromagnetic (EM) methods measure how the subsurface conducts electrical current, making them well-suited for detecting conductive ore bodies. Magnetotelluric (MT) surveying, an example of such methods, records natural electromagnetic signals at the surface. For 1D MT inversion, the input is a set of apparent resistivity and phase measurements recorded at multiple frequencies, and the goal is to predict how electrical conductivity varies with depth. Saibi et al. [74] compared recurrent (LSTM, GRU) and attention-based (Informer, a Transformer variant) architectures for this task, finding that recurrent models achieved slightly better accuracy on both synthetic and field data.

3.2.3. Physics-Informed and Operator-Learning Methods

The methods described in Sections 3.2.1 and 3.2.2 learn the inverse mapping purely from data. An alternative approach is to embed the governing physical equations directly into the network. Physics-Informed Neural Networks (PINNs) [13] add a physics residual to the loss function, penalizing solutions that violate known equations. PINNtomo [14] applies this idea to seismic tomography, constraining the network to satisfy the Eikonal equation while fitting observed travel-time data.

A related direction replaces expensive numerical simulators with learned surrogate models. Neural operators learn to map between function spaces, enabling fast approximate solutions to partial differential equations. GP-cubed [75] uses neural operators as surrogate forward models for geophysical simulation, accelerating inversion workflows. Yang et al. [76] applied the Fourier Neural Operator (FNO) [77] to seismic wave propagation, approximating wave-equation solutions at a fraction of the computational cost of conventional solvers.

 doi:10.20944/preprints202607.2303.v1

3.3. Geochemical Analysis

Geochemical data consist of element concentration measurements obtained from rock samples, drill cores, stream sediments, or soil surveys [56]. These data are inherently tabular: each sample is described by concentrations of tens of elements. The main ML tasks are anomaly detection (finding unusual element patterns that may indicate nearby ore; Section 3.3.1), classification (distinguishing productive from barren geological systems; Section 3.3.2), and regression (estimating physical conditions such as temperature and pressure from mineral compositions; Section 3.3.3).

3.3.1. Geochemical Anomaly Detection

Regional geochemical surveys produce large tabular datasets. The goal is to identify spatial locations with unusual element concentrations that may indicate hidden mineral deposits. A key challenge is that background geochemistry varies spatially, so a fixed threshold will produce false positives in some regions and miss anomalies in others. The Deep Autoencoder Network connected to Geographical Random Forest (DAN-GRF) [15] addresses this by combining the representation learning of deep autoencoders with the spatial awareness of geographical random forests [78], adapting anomaly thresholds to local geochemical context. For multi-element rare earth element (REE) datasets, deviation networks [79] have been applied to detect anomalies in high-dimensional geochemical compositions [80].

3.3.2. Mineral Classification and Fertility Prediction

Certain minerals preserve chemical signatures of the geological environment in which they formed. If that environment is associated with ore formation, these signatures can serve as exploration indicators [57]. Zircon, a common accessory mineral, is widely studied because its trace element composition varies depending on whether the host rock is associated with a mineral deposit. This is essentially a tabular classification task: given a vector of trace element concentrations, predict whether the sample comes from an ore-bearing or barren system. ML models have been trained to quantify these discriminating criteria for porphyry copper deposits [81], while XGBoost and LightGBM have been applied to predict deposit type and resource size from zircon chemistry [82]. Broader classification of igneous rock types from zircon trace elements has also been demonstrated in [83].

3.3.3. ML-Based Thermobarometry

Thermobarometry estimates the temperature and pressure at which a mineral formed, based on its chemical composition [84]. This is a regression task: given a vector of oxide concentrations from a mineral grain, predict the formation conditions. A recent workflow [84] enhances ML-based thermobarometry for clinopyroxene (a common rock-forming mineral), using tree-based ensembles with Monte Carlo error propagation and bias correction to improve prediction reliability over previous ML and classical calibrations. A related regression task is estimating paleo-crustal thickness from whole-rock geochemistry. ML-based "Mohometry" [55] trains Random Forests and Gradient Boosting Machines on 66 geochemical proxies from igneous rock samples to predict Moho depth at the time of magma formation, enabling the reconstruction of crustal thickness evolution across diverse tectonic settings.

3.4. Remote Sensing and Hyperspectral Analysis

Remote sensing provides multi-spectral and hyperspectral observations of the Earth's surface. In mineral exploration, these data support three main tasks: lithological mapping (Section 3.1), identification of alteration zones (areas where hot subsurface fluids have changed the original rock mineralogy, often indicating nearby ore), and mapping of geological structures such as faults and folds that control fluid flow and mineral deposition [59]. This section focuses on the latter two.

ML methods for these tasks operate at two spectral resolutions. With multi-spectral imagery, CNNs have been applied to identify alteration signatures [16]. Hyperspectral data, which capture detailed spectral information across hundreds of narrow bands [85], enable finer mineral discrimination.

SpecPool-Transformer [17], a ViT-based model with spectral pooling, was designed specifically for mapping alteration minerals from hyperspectral data. Since individual pixels often contain mixtures of several minerals, hyperspectral unmixing methods decompose mixed spectra into constituent mineral signatures and their proportions [86]. Rev-Net [87] addresses this with reversible generative networks that account for spectral variability across a scene.

The Segment Anything Model (SAM) [88] has been adapted for geospatial applications through segment-geospatial [89], enabling zero-shot segmentation of geological features, alteration zones, and land cover classes from satellite and aerial imagery.

4. Mineral Prospectivity Mapping

The domain-specific methods reviewed in Section 3 each produce processed data products: lithological classifications from geological mapping, subsurface property models from geophysical inversion, anomaly scores from geochemical analysis, and alteration or mineral maps from remote sensing. In MPM, these products serve as evidence layers, each capturing one aspect of the geological environment; for each grid cell, the values across all layers form the input used to predict which areas are most likely to host mineral deposits [4,53]. This section reviews MPM methods; the cross-cutting challenges of spatial autocorrelation, class imbalance, and uncertainty quantification that affect MPM and other geoscience ML tasks are discussed in Section 7. It is organized as follows. After defining the problem formulation (Section 4.1), we cover classical and ensemble methods (Section 4.2), then deep learning approaches organized by the methodological challenge they address (Section 4.3). We then discuss transfer learning across geological regions (Section 4.4) and 3D prospectivity mapping (Section 4.5), and close with a summary of open gaps. Table 3 summarizes the methods reviewed in this section, and Figure 3 provides a chronological overview.

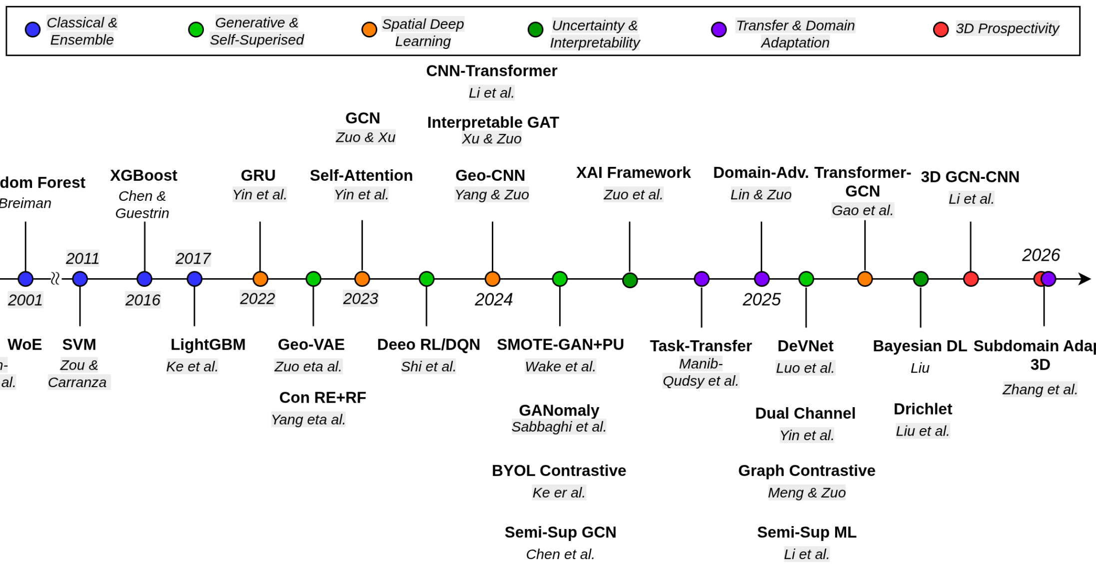

Figure 3. Chronological overview of ML methods for mineral prospectivity mapping, from classical statistical approaches (1989–2017) through the rapid expansion of deep learning methods (2022–present). Methods are color-coded by category (see legend).

4.1. Problem Formulation and Workflow

MPM can be formulated as a spatial classification or regression problem [4,53]. The inputs are multi-layer geoscientific evidence maps, derived from geological, geophysical, geochemical, and remote sensing data [21,22], and the outputs are spatial predictions of mineralization favorability. Known mineral deposit locations serve as positive training samples, while the labeling of non-deposit locations presents a fundamental challenge [6] (see Section 7). The general workflow involves: **(1)** compilation and pre-processing of evidence layers, **(2)** feature engineering or representation learning, **(3)** model training and evaluation with appropriate spatial validation [8], and **(4)** generation of prospectivity maps with uncertainty estimates [90].

4.2. Classical and Ensemble Methods

The earliest data-driven approaches to MPM employed statistical methods such as Weights of Evidence (WoE) [18] and logistic regression. These were subsequently complemented by ensemble tree methods, particularly Random Forests (RF) [19], which became the most widely used ML algorithm for MPM due to their ability to handle mixed data types, implicit feature selection, and robustness to overfitting [22].

Support Vector Machines (SVMs) [91,92] have also been extensively applied, particularly for binary classification of prospective vs. non-prospective areas.Gradient boosting methods (XGBoost [93], LightGBM [94]) have gained popularity for their strong performance on tabular geoscience data.

4.3. Deep Learning Approaches

Deep learning methods are increasingly applied to MPM. We organize them by the methodological challenge each addresses, rather than by architecture alone, to clarify where different approaches contribute.

4.3.1. Spatial Feature Learning

A central question in MPM is how to represent evidence layers for prediction. Methods range from treating each grid cell independently to explicitly modeling spatial structure. We organize them below by the degree of spatial context they incorporate.

Per-cell methods. The simplest deep learning approach extracts a feature vector of evidence layer values at each grid cell and classifies it with a fully connected network, entirely ignoring spatial structure. Yin et al. [95] treated the evidence layers at each cell as an ordered sequence and applied Gated Recurrent Units (GRUs) to capture inter-layer dependencies, though without spatial context from neighboring cells. Yin et al. [96] proposed a self-attention model that learns pairwise relationships among evidence layer features at each cell, weighting different geological inputs adaptively.

CNNs. CNNs move beyond per-cell classification by extracting local image patches around each cell, learning spatial patterns from the surrounding geological context. Yang and Zuo [97] embedded geological domain knowledge into CNN training through both a geology-based loss penalty and architectural modifications that encode known spatial relationships between deposits and ore-controlling structures.

Graph neural networks (GNNs). GNNs represent cells as nodes in a spatial graph, with edges connecting nearby cells. Zuo and Xu [98] introduced graph deep learning for MPM, using a distance threshold to define edges and comparing Graph Convolutional Network (GCN) and Graph Attention Network (GAT) architectures. Xu and Zuo [99] extended this with an interpretable GAT that incorporates geological knowledge into the graph topology by removing edges that cross fault lines or lithological boundaries.

Hybrid architectures. Each of the above representations captures a different aspect of the evidence data: CNNs extract local spatial patterns, GNNs model spatial relationships through a graph structure, and per-cell methods learn inter-feature dependencies. Hybrid architectures combine two or more of these strategies to operate at multiple scales simultaneously. Li et al. [100] combined CNNs with transformers [101], using convolutions for fine-grained local features and self-attention for longer-range geological context. Gao et al. [102] fused a transformer encoder with a GCN, but over a geochemical element correlation graph rather than a spatial graph: nodes represent elements, edges encode statistically significant inter-element correlations, the transformer provides global attention across elements, and the GCN refines representations through local graph aggregation.

 doi:10.20944/preprints202607.2303.v1

4.3.2. Learning with Scarce and Ambiguous Labels

The extreme scarcity of known deposits, combined with the fundamentally unlabeled nature of non-deposit locations (Section 7), motivates several learning paradigms beyond standard supervised classification.

Generative models. GANs [20] and Variational Autoencoders (VAEs) have been applied to MPM in three roles: synthetic data augmentation to address label scarcity, anomaly-based prospectivity detection, and direct prospectivity scoring. Wake et al. [21] used a SMOTE-GAN pipeline to synthesize positive training samples for lateritic Ni-Co prospectivity, combining the augmented data with positive-unlabeled bagging to derive reliable negative labels, followed by Random Forest classification. Sabbaghi et al. [103] adapted GANomaly [104] for anomaly-based prospectivity detection, adding a geological constraint loss based on the spatial correlation between mineralization and ore-controlling structures, and training on frequency-domain geochemical data obtained via 2D Fourier transform. Zuo et al. [105] used a geologically constrained VAE whose reconstruction probability serves directly as a prospectivity score, with a power-law spatial correlation loss encoding known relationships between deposits and geological controlling features.

Self-supervised and semi-supervised learning. Miao et al. [106] applied BYOL [107] contrastive pre-training on unlabeled geochemical raster patches before fine-tuning on limited deposit labels, yielding more discriminative features than purely supervised training. Meng and Zuo [108] combined contrastive pre-training with graph neural networks, reducing dependence on labeled deposits. Semi-supervised graph convolutional networks [109] propagate labels to unlabeled cells through the spatial graph structure. Li et al. [110] further explored semi-supervised strategies for MPM, showing that semi-supervised methods, including a novel GAN-based approach (SemiGAN), outperformed supervised baselines in capturing known deposits within high-potential areas.

Unsupervised representation learning. Yang et al. [111] used convolutional autoencoders for unsupervised feature extraction followed by Random Forest classification, decoupling representation learning from label-dependent prediction.

4.3.3. Uncertainty, Interpretability, and Alternative Paradigms

The methods described in Sections 4.3.1 and 4.3.2 focus on improving prediction accuracy. This section covers three complementary concerns: quantifying prediction confidence, explaining model decisions, and alternative learning formulations.

Uncertainty quantification. Quantifying prediction uncertainty is important for exploration decisions, as it distinguishes areas of low mineral potential from areas where predictions are unreliable due to limited data. Liu [90] proposed a Bayesian deep learning framework that produces both prospectivity predictions and uncertainty maps. Liu et al. [112] took an evidential approach, using a Dirichlet-based network that outputs a distribution over class probabilities in a single forward pass, decomposing uncertainty into aleatoric (data noise) and epistemic (model ignorance) components without requiring ensemble training or Monte Carlo sampling.

Explainability. Zuo et al. [113] proposed a framework for explainable AI in MPM, reviewing techniques including feature map visualization, gradient-based attribution methods such as Grad-CAM [114], and SHAP-based feature importance analysis. Zhang et al. [115] used an LLM (Qwen2-72B) with retrieval-augmented generation to extract geological knowledge from published literature into a knowledge graph, then mined the graph to select geochemically interpretable features for gcForest-based prospectivity prediction, where each selected feature can be traced back to its source literature. Yin et al. [116] coupled a CNN with SHAP in an iterative semi-supervised loop: at each iteration, the CNN expands its labeled set via pseudo-labeling while SHAP values update feature weights for the next iteration, making interpretability an integral part of model refinement rather than a post-hoc analysis. Luo et al. [117] applied DevNet, a semi-supervised anomaly detection network requiring only

 doi:10.20944/preprints202607.2303.v1

a few labeled deposit samples, to multi-source exploration data (geological, geophysical, geochemical, and remote sensing) with Kernel SHAP for post-hoc feature importance validation.

Reinforcement learning. Shi et al. [118] framed prospectivity mapping within a Deep Q-Network (DQN) framework, where each pixel's geochemical and geological features define a state and the agent outputs a binary mineralization potential action. The reward combines a supervised signal from known deposits with an unsupervised exploration reward based on Isolation Forest anomaly scores, enabling the model to leverage both labeled and unlabeled data.

4.4. Transfer Learning and Domain Adaptation

Transfer learning and domain adaptation aim to leverage knowledge from data-rich settings (e.g., well-explored regions or related geological tasks) to improve predictions in data-scarce target settings, reducing the need for costly labeled samples in new areas. Frontier exploration areas typically have little to no labeled data, making transfer learning a natural strategy. Existing work spans three transfer strategies: task transfer within a study area, cross-region domain adaptation, and self-supervised pre-training.

Task transfer. Transfer prospectivity learning [23] uses a pretext geological classification task to pre-train representations, then transfers them to the prospectivity prediction task within the same study area, reducing dependence on scarce deposit labels.

Cross-region domain adaptation. Lin and Zuo [119] proposed an improved domain adversarial neural network that combines adversarial training with Maximum Mean Discrepancy (MMD) alignment to learn domain-invariant features, enabling knowledge transfer between geologically distinct regions. Zhang et al. [120] extended domain adaptation to 3D MPM, using class-weighted local MMD to align fine-grained subdomain distributions and prevent the rare ore-body class from being overwhelmed by the dominant barren class during adaptation.

Self-supervised pre-training. Daruna et al. [121] applied masked image modeling to pre-train a backbone network on unlabeled multi-modal geospatial data, then fine-tuned it for MPM. The approach was evaluated on lead-zinc deposits across North America and Australia, demonstrating that self-supervised pre-training on geospatial data improves prospectivity predictions over training from scratch.

4.5. 3D Prospectivity Mapping

Three-dimensional MPM extends traditional 2D surface-based approaches to predict mineralization potential at depth. As near-surface deposits become scarcer, exploration increasingly requires targeting below cover, making 3D prediction a growing priority. The main ML challenge is handling sparse, irregularly sampled volumetric data across large 3D domains.

Hybrid architectures. Li et al. [24] proposed a 3D GCN–CNN hybrid that uses graph convolutional networks to capture irregular geological topological relationships and CNNs to extract spatial features from voxelized data. Xie et al. [122] combined 3D CNNs with a transformer encoder for local and global feature extraction, introducing a spatial continuity loss that penalizes abrupt changes in predicted feature maps across the x, y, and z directions, encouraging geologically coherent predictions.

Uncertainty quantification. Zhang et al. [123] addressed uncertainty for 3D MPM using a random forest framework with entropy-based uncertainty decomposition into aleatoric and epistemic components and Bayesian hyperparameter optimization, enabling selective targeting of high-confidence subsurface predictions. Domain adaptation methods for 3D MPM, including class-weighted subdomain alignment, are discussed in Section 4.4.

Table 3 provides a comparative summary of the ML methods applied to MPM, organized to mirror the subsections above: spatial feature learning (Section 4.3.1), scarce and ambiguous labels (Section 4.3.2), uncertainty and interpretability (Section 4.3.3), transfer learning (Section 4.4), and 3D

 doi:10.20944/preprints202607.2303.v1

mapping (Section 4.5). A cross-cutting distinction is how each method represents the evidence layers: *tabular (per-cell)* methods classify each grid cell independently from its feature vector, *image patch* methods extract local raster windows to learn spatial patterns, and *graph-based* methods model cells as nodes connected by spatial or geological relationships.

Table 3. Comparison of ML methods for MPM. *Input Repr.*: Tab. = tabular feature vector per cell, Img. = local image patches, Seq. = sequential. *Modalities*: Ge = geological (incl. structural), Gp = geophysical, Gc = geochemical, RS = remote sensing. *Output*: Prob. = probability/favorability map, Unc. = uncertainty map, Anom. = anomaly score, Class. = classification map. Polymet. = polymetallic. Entries marked — denote general-purpose methods without a specific case study.

Method	Input Repr.	Modalities	Output	Case Study	Ref.
Classical and Ensemble Methods					
WoE	Tab. (per-cell)	—	—	—	[18]
Random Forest	Tab. (per-cell)	Ge, Gp, RS	Prob.	Gawler, AU: Co-Cr-Ni	[22]
SVM + SMOTE	Tab. (per-cell)	Ge, Gp	Prob.	Carajás, Brazil: Cu-Au	[124]
XGBoost / LightGBM	Tab. (per-cell)	—	—	—	[93,94]
Spatial Feature Learning					
GRU	Tab. (seq.)	Ge	Prob.	—	[95]
Self-Attention	Tab. (per-cell)	Ge, Gc	Prob.	—	[96]
CNN	Img. (pixel)	RS	Class.	Broken Hill, AU: alteration	[16]
Geo-Constr. CNN	Img. patches	Ge, Gp, Gc	Prob.	—	[97]
Graph DL	Graph	Ge	Prob.	—	[98]
Interp. GAT	Graph	Ge, Gc	Prob.	SW Fujian, China: Fe polymet.	[99]
CNN-Transformer	Multi-sc. raster	Ge, Gp, Gc	Prob.	S. Xing'an, China: Sn	[100]
Trans.-GCN Fusion	Element graph	Gc	Prob.	Guangdong, China: Pb-Zn	[102]
Scarce and Ambiguous Labels					
GAN + PU Bag. + RF	Tab. + GLCM	Ge, Gp, RS	Prob.	Lachlan, AU: Ni-Co	[21]
GANomaly	Tab. (per-cell)	Gc	Anom.	—	[103]
Geo-Constr. VAE	Tab. (per-cell)	Ge	Prob.	—	[105]
Conv. AE + RF	Img. patches	Ge, Gc	Prob.	—	[111]
Self-sup. (BYOL)	Img. patches	Gc	Prob.	Malanyu, China: Au	[106]
Self-sup. GCN	Graph	Ge, Gc	Prob.	SW Fujian, China: Fe polymet.	[108]
Semi-sup. GCN	Graph	Ge, Gp, Gc	Prob.	E. Kunlun, China: polymet.	[109]
Semi-sup. ML	Tab./Img.	Ge, Gp, Gc	Prob.	Nanling, China: W-Sn	[110]
Uncertainty, Interpretability, and RL					
Bayesian DL	Tab. (per-cell)	Ge, Gc	Prob.+Unc.	Nanling, China: W-Sn	[90]
Dirichlet DL	Tab. (per-cell)	Ge, Gp, Gc	Prob.+Unc.	Zhongtiaoshan, China: Cu	[112]
LLM+KG+gcForest	Tab. (per-cell)	Gc	Class.	Nanling, China: rare metals	[115]
Dual-Channel CNN	Img. patches	Ge, Gc, RS	Prob.	Keeryin, China: Li	[116]
DevNet (DEEP-SEAM)	Tab. (per-cell)	Ge, Gp, Gc, RS	Anom.	Curnamona, AU: REE	[117]
Deep RL (DQN)	Tab. (per-cell)	Ge, Gc	Prob.	—	[118]
Transfer Learning and Domain Adaptation					
Transfer DNN	Tab. (per-cell)	Ge, Gp, Gc	Prob.	Yukon, Canada: porphyry Cu	[23]
Domain Adv. NN	Tab. (per-cell)	Ge, Gc	Prob.	—	[119]
Deep Subdomain Adapt.	3D voxel	Ge, Gp	Prob.	Damiao, China: Fe-V-Ti	[120]
GFM4MPM	Multi-modal raster	Ge, Gp	Prob.+Unc.	N. America + AU: Pb-Zn	[121]
Text-Derived Features					
NLP + Word Vectors	Text-derived	Ge (text)	Prob.	Canada/US/AU: Zn-Pb MVT	[36]
LLM + Transformer	Text + Tab.	Ge (text), Gp, Gc	Prob.	Canada: Zn-Pb MVT	[125]
3D Prospectivity Mapping					
3D GCN-CNN	3D vox. + graph	Ge, Gp, Gc	Prob. (3D)	E. Chating, China: Cu-Au, Cu-W polymet.	[24]
3D CNN-Trans.	3D voxel	Ge, Gc	Prob. (3D)	—	[122]
3D UQ-RF	3D voxel	Ge, Gp	Prob.+Unc.	Wulong, China: Au	[123]

4.6. Summary and Open Gaps

Several patterns emerge from this review of MPM methods (Table 3). The majority of studies operate on tabular per-cell features, classifying each grid cell independently without spatial context. Graph-based and image-patch methods that explicitly model spatial structure remain a minority. Nearly all deep learning studies address a single commodity in a single study area, making cross-study comparison difficult in the absence of shared benchmarks. Transfer learning across geological regions has been attempted by only a handful of studies, despite being central to practical exploration, where target areas are by definition data-sparse. Uncertainty quantification accompanies only a small fraction of the reviewed methods, and 3D prospectivity mapping at depth remains at its early stages, with most work confined to 2D surface-based prediction. These challenges and the corresponding research directions are discussed in Section 7.

 doi:10.20944/preprints202607.2303.v1

5. Foundation Models and Knowledge Extraction for Mineral Exploration

The gaps identified in the previous sections, particularly label scarcity (Section 4.3.2), limited transferability (Section 4.4), and modality-specific training (Section 3), motivate the adoption of foundation models [25], i.e., large-scale models pre-trained on broad datasets that produce general-purpose representations adaptable to downstream tasks through fine-tuning or prompting. This section reviews foundation models that have emerged across geoscience domains, together with the NLP extraction tools (word embeddings, named entity recognition, knowledge graphs) that convert unstructured geological text into structured inputs for exploration workflows.

No single foundation model currently spans the full range of modalities used in mineral exploration: satellite imagery, geophysical grids, geochemical assays, geological maps, and unstructured text. However, foundation models now exist in several of these domains individually: EO models for satellite imagery [27], seismic foundation models for geophysical data [28], geoscience LLMs for text [30], and vision–language models for map interpretation [126]. Each addresses a subset of the mineral exploration data stack. The central opportunity is not any single model, but connecting these domain-specific building blocks into integrated exploration workflows.

The gaps identified in the MPM review (Section 4) provide a concrete lens for assessing how close these building blocks are to practical use. We organize them into three maturity tiers:

Demonstrated (proof-of-concept exists).

- Self-supervised pre-training can address label scarcity and cross-region generalization. GFM4MPM [121] used masked image modeling on multi-modal geospatial data to learn transferable representations, evaluating prospectivity prediction across North America and Australia, though it builds a custom pipeline rather than adapting an established EO foundation model.
- NLP and LLMs can convert geological text into quantitative evidence layers for prospectivity prediction. Three studies [36,115,125] have demonstrated this end-to-end pathway.

Architecturally ready (models exist, not yet applied to exploration).

- Multi-modal foundation models could address the single-modality limitation. DOFA [127] uses wavelength-conditioned hypernetworks to jointly encode optical, SAR, and hyperspectral inputs, while Terramind [128] extends this to optical, SAR, DEM, and text through an any-to-any generative framework. Neither has ingested the geophysical grids or geochemical assays central to mineral exploration.
- Vision–language models could support geological map interpretation. PEACE [126] benchmarks VLM comprehension of geologic maps, but its outputs have not been connected to quantitative prospectivity pipelines.

Open (no foundation model capability exists yet).

- Uncertainty quantification for foundation model outputs remains unexplored in this domain.
- No agentic system currently orchestrates across modalities for mineral exploration workflows.

The subsections that follow review the current state of each building block, organized by modality (Table 4).

Table 4. Foundation models and NLP tools relevant to mineral exploration, organized by modality.

Model	Modality	Organization	Architecture	Key Features
Earth Observation				
Clay [26]	Satellite imagery	Clay Foundation	MAE-based	Open-source; multi-sensor; location-aware
Prithvi [27]	HLS imagery	IBM + NASA	ViT-based MAE	Temporal embeddings; open weights
SpectralGPT [129]	Spectral RS	Hong et al.	3D tokenization MAE	Spatial-spectral structure preservation
DOFA [127]	Multi-sensor	Zhu X-Lab	Dynamic hypernetwork	Wavelength-conditioned; sensor-agnostic
SkySense [130]	Optical + SAR	Ant Group	Factorized encoder	21.5M temporal sequences; multi-modal
Terramind [128]	Multi-modal	IBM Research	Any-to-any Transformer	Generative; optical, SAR, DEM, text
TerraFM [131]	Sentinel-1/2	MBZUAI	ViT + cross-attention	Modality-as-augmentation; DINO-based
ScaleMAE [132]	Satellite imagery	Reed et al.	MAE	Scale-aware; GSD-conditioned
SatMAE++ [133]	Multi-spectral	Noman et al.	MAE	Multi-spectral ViT pre-training
Geophysics				
Guo et al. [134]	Geophysical data	Guo et al.	DINOv2 + LoRA	CV-to-geophysics transfer; few-shot
SeismicFM [28]	Seismic data	Sheng et al.	ViT-based MAE	2.3M seismic images; 192 3D volumes
GEM3D [29]	Seismic 3D	Wu et al.	CNN (HRNet)	Physics-informed; promptable; zero-shot
Language and Knowledge Extraction				
K2 [30]	Geoscience text	Deng et al.	LLM (LLaMA-7B)	5.5B tokens; geoscience QA
GeoGalactica [31]	Geoscience text	Geobrain AI	LLM (Galactica-30B)	65B tokens; geoscience NLP tasks
JiuZhou [32]	Geoscience text	THU-ESIS	LLM (Mistral-7B)	Two-stage pre-adaptation; open weights
GeoMinLM [135]	Mining/geology text	Fu et al.	LLM (Baichuan-2)	Region-specific (Yunnan); mineral KG
MetalGPT [136]	Mining text	NN-Tech	LLM	Mining and metallurgy
PetroMind [63]	Rock imagery + text	Chen et al.	VLM (Qwen2.5-VL)	Rock classification; SA-Rock metric
GeoBERT [34]	Geological text	Liu et al.	BERT + BiLSTM-CRF	Geological NER with limited labels
Vision–Language				
PEACE [126]	Geologic maps	Microsoft + CAGS	MLLM (GPT-4o)	Benchmark + agentic QA for maps
EarthScape [137]	Surficial geology	Massey et al.	Dataset	Aerial imagery, DEM, terrain features
SatCLIP [138]	Location–image	Klemmer et al.	CLIP-style	Coordinate-to-feature; no image at inference
Agentic AI				
Earth-Agent [139]	EO multi-modal	–	ReAct + MCP	104 tools; multi-step EO workflows
OpenEarthAgent [140]	EO multi-modal	–	Qwen3-4B + tools	Unified tool registry; validated trajectories

5.1. Earth Observation (EO) Foundation Models

Self-supervised EO foundation models learn general-purpose representations from large unlabeled satellite archives, reducing dependence on task-specific labels. For mineral exploration, the key question is whether these representations — learned primarily from optical and SAR imagery — can extend to the geophysical grids and hyperspectral data that dominate exploration workflows.

MAE-based models.

Clay [26] is an open-source model trained using a Masked Autoencoder (MAE) [141] on diverse satellite data, with location-aware encoding and multi-sensor support. Prithvi [27], developed by IBM and NASA, is trained on Harmonized Landsat-Sentinel (HLS) data [142] using a ViT [143] with temporal embeddings and open weights. ScaleMAE [132] incorporates ground sample distance into positional encodings to learn scale-aware representations, while SatMAE++ [133] explores multi-spectral pre-training strategies for ViTs. These models demonstrate that self-supervised pre-training on satellite imagery produces transferable representations, though their pre-training data are limited to optical and SAR bands from Sentinel missions.

 doi:10.20944/preprints202607.2303.v1

Spectral models.

SpectralGPT [129] targets spectral remote sensing data specifically, using 3D tokenization to preserve spatial-spectral structure across input bands. Mineral alteration mapping relies on diagnostic absorption features in specific wavelength ranges (e.g., 2.0–2.5 μm for clay minerals [85]), and SpectralGPT's spectral pre-training aligns with this requirement. However, it has been pre-trained on Sentinel-2 imagery (13 bands) rather than the airborne hyperspectral sensors (200+ bands) typically used in detailed exploration surveys.

Multi-modal and multi-sensor models.

Dynamic One-For-All (DOFA) [127] uses a wavelength-conditioned dynamic hypernetwork to handle arbitrary sensor modalities through a single architecture, including multi-spectral, SAR, and hyperspectral inputs. Terramind [128] introduces an any-to-any generative framework capable of generating or predicting across optical imagery, SAR, digital elevation models, and text. TerraFM [131] and SkySense [130] provide further multi-sensor architectures; SkySense was pre-trained on 21.5 million multi-modal temporal sequences using a factorized spatiotemporal encoder.

Despite this modality gap, EO foundation models represent a mature building block: open weights, established fine-tuning frameworks (e.g., Terratorch [144]), and self-supervised pre-training strategies applicable to exploration-relevant tasks such as alteration mapping and lithological classification.

5.2. Geophysical Foundation Models

Geophysical surveys (gravity, magnetics, electromagnetics) are central to mineral exploration [3], yet foundation model development in geophysics has focused almost entirely on seismic data, driven by the oil and gas industry.

Guo et al. [134] adapt DINOv2 via LoRA fine-tuning for geophysical segmentation tasks, demonstrating that representations learned from natural images can transfer to seismic facies classification, fault detection, and salt body identification with as few as 50 labeled samples. SeismicFM [28] is a self-supervised ViT pre-trained via masked autoencoders on 2.3 million 2D seismic images from 192 globally collected 3D volumes, adaptable to downstream tasks including facies classification, geobody segmentation, inversion, denoising, and interpolation. Notably, the largest share of its training data comes from the South Australian Resources Information Gateway (SARIG), providing a connection to mineral exploration data infrastructure. GEM3D [29] proposes a physics-informed, promptable foundation model for unified subsurface understanding from seismic data, targeting structural interpretation, stratigraphic analysis, geobody segmentation, and physical property modeling, with demonstrated zero-shot generalization to unseen geological settings.

No foundation model yet exists for gravity, magnetic, or electromagnetic survey data, the dominant geophysical methods in mineral exploration. National geological survey archives (Section 6) already provide large-scale coverage for these modalities, making the assembly of a pre-training corpus feasible but not yet attempted.

5.3. Language Models and Knowledge Extraction

Most MPM studies rely exclusively on numerical evidence layers: geophysical grids, geochemical assays, and categorical geological maps (Table 3). Yet mineral exploration generates vast quantities of text, including field notes, exploration reports, scientific publications, drillhole logs, and government survey records, that encode critical domain knowledge not captured in these numerical inputs. Two complementary approaches unlock this textual modality. Foundation LLMs pre-trained on geoscience corpora can reason about geological concepts and answer domain questions. Targeted NLP tools, including word embeddings, Named Entity Recognition (NER), and knowledge graphs, extract structured information from unstructured text. Both feed into the broader goal of converting textual geological knowledge into quantitative inputs for exploration workflows. We first review geoscience

 doi:10.20944/preprints202607.2303.v1

LLMs (Section 5.3.1), then targeted NLP tools (embeddings, NER, knowledge graphs; Sections 5.3.2 and 5.3.3), and finally their integration into prospectivity prediction (Section 5.3.4).

5.3.1. Geoscience Large Language Models

Several LLMs have been adapted for geoscience through domain-specific pre-training or fine-tuning. K2 [30] further pre-trains LLaMA-7B on 5.5 billion tokens of geoscience text, demonstrating improved performance on geoscience question-answering compared to general-purpose LLMs. GeoGalactica [31] extends Galactica [145] with 65 billion tokens of geoscience text and supervised fine-tuning, targeting geoscience NLP tasks including knowledge graph construction and question answering. JiuZhou [32] introduces a two-stage pre-adaptation framework that first trains on general text before specializing on geoscience data, with open model weights and training corpus. Two models target the mineral resources domain directly. GeoMinLM [135] fine-tunes Baichuan-2 on geological reports and a mineral deposit knowledge graph specific to Yunnan Province, demonstrating the value of region-specific adaptation for geological question answering. MetalGPT [136] addresses the specialized language of mining and metallurgy. PetroMind [63] takes a multimodal approach, adapting Qwen2.5-VL with LoRA for rock image classification and lithological description generation. Lithological identification is a fundamental upstream task for geological mapping that directly supports mineral exploration, and PetroMind introduces SA-Rock, an LLM-based metric for evaluating the quality of generated rock descriptions.

5.3.2. Domain-Specific Embeddings and Information Extraction

Beyond foundation LLMs, targeted NLP tools extract structured information from geological text at finer granularity.

Word embeddings.

Foundational word embedding methods such as Word2Vec [146] and GloVe [147], trained on geoscience corpora, capture semantic relationships between geological concepts in vector space. GeoVec [33], trained on geoscience publications from Elsevier ScienceDirect, encodes domain-specific relationships where vector arithmetic reflects known associations such as rock type classification and metamorphic grade sequences. GeoVectoLitho [148] applies GeoVec embeddings with an MLP classifier and spatial interpolation to produce 3D lithological maps from free-text borehole descriptions. Linphrachaya et al. [149] explore whether GloVe embeddings combined with dimensionality reduction can provide geographic pointers to lithium deposits from geological survey text, though prediction errors remain large. Intrinsic evaluation benchmarks [150] confirm that domain-retrained GloVe and BERT models outperform generic counterparts on geoscience-specific analogy, clustering, and relatedness tasks.

Named entity recognition and information extraction.

GeoBERT [34] adapts Chinese BERT with continued pretraining on geological thesauruses, then applies BiLSTM-CRF [151] for NER on geological text, recognizing entities such as rock types, minerals, strata, and locations with limited labeled data. OzRock [152] provides a labeled NER dataset for the mineral exploration domain, enabling training and evaluation on Australian geological text. Dimeski and Rahimi [60] use Bi-LSTM-CRF and BERT sequence labeling to extract structured drillhole results (hole ID, depth, grade) from ASX-listed mining company reports. Dong et al. [61] address the complementary challenge of extracting structured data from tables in geological reports, combining improved Mask R-CNN for cell recognition with NER to construct geological knowledge graphs.

5.3.3. Knowledge Graphs for Geoscience

Knowledge graphs [153] provide structured representations of geological entities and their relationships. GeoERE-Net [154] performs joint entity and relation extraction on geological reports using a CasRel-based architecture with RoBERTa [155], BiLSTM [156] with axial attention, and graph convolu-

 doi:10.20944/preprints202607.2303.v1

tion, extracting triples that encode stratigraphic and lithological relationships. StraKG [35] constructs stratigraphic knowledge graphs linking strata to rock types and spatial locations. Ma [157] provides a comprehensive review of knowledge graph construction and application across the geosciences.

5.3.4. Text-Derived Features for Prospectivity Mapping

The tools described in Sections 5.3.1, 5.3.2, and 5.3.3 form a pipeline whose value for mineral exploration is realized when text-derived features are integrated into prospectivity prediction. Three recent studies demonstrate this end-to-end pathway: **Lawley et al. [36]** applied a geoscience-retrained GloVe [147] model to text from geological map databases across Canada, the United States, and Australia, encoding map polygon descriptions as continuous feature vectors. Using Naive Bayes classifiers on these vectors, they predicted Zn-Pb MVT and clastic-dominated deposit locations, showing that unstructured geological text alone can serve as a spatial input for prospectivity modeling. **Zhang et al. [115]** used Qwen2-72B-instruct [158] with structured prompts to extract geological knowledge from 43 published papers into a domain-specific knowledge graph for rare metal deposits. The graph was mined to rank element importance and select geochemically interpretable features for gcForest-based prospectivity prediction, where each selected feature can be traced back to its source literature. **Parsa et al. [125]** fine-tuned BERT [159] on geoscience text to generate embeddings for 1.8 million hexagonal cells across Canada, then fed these embeddings together with geophysical and geochronological features into a self-supervised transformer trained via masked regression. The combined model reduced the search space by 87% for Zn-Pb MVT deposits, demonstrating how text-derived features can complement traditional numerical evidence layers.

Together with GFM4MPM [121], which applies masked image modeling on multi-modal geospatial data for prospectivity prediction (Table 3), these studies represent the few cases where foundation model concepts have been directly applied to mineral exploration.

5.4. Vision–Language Models

PEACE [126] introduces a benchmark and agentic QA system for geologic map comprehension, using GPT-4o [160] with hierarchical map decomposition and domain knowledge injection to answer questions about map content such as scale extraction, legend interpretation, and lithology identification. EarthScape [137] provides the first multimodal dataset for surficial geologic mapping, combining aerial imagery, DEMs, terrain-derived features, and geological annotations for classification of surface materials. SatCLIP [138] learns general-purpose location encodings by training a lightweight coordinate encoder against a Sentinel-2 image encoder via contrastive learning. At inference, only coordinates are needed, producing feature vectors that capture environmental and land-use characteristics and support geographic generalization to unseen regions.

5.5. Agentic AI

Agents extend foundation models from static inference to autonomous, multi-step reasoning by invoking external tools, querying databases, and chaining operations across modalities.

Earth-Agent [139] pairs an LLM controller with 104 specialized tools organized via the Model Context Protocol (MCP), using a ReAct-style [161] loop to autonomously execute multi-step EO workflows across RGB imagery, spectral data, and derived products. OpenEarthAgent [140] provides a complementary framework with a unified tool registry spanning perception, GIS computation, spectral analysis, and georeferenced raster operations, fine-tuning Qwen3-4B [162] on validated multi-step reasoning trajectories. Both frameworks demonstrate that LLM-based agents can orchestrate cross-modal geospatial analysis. Of the building blocks reviewed in Sections 5.1, 5.2, 5.3, 5.4, and 5.5, only the text-to-prospectivity pathway has demonstrated end-to-end integration with mineral exploration [36, 115,125]. EO foundation models offer mature infrastructure (open weights, fine-tuning frameworks) but remain untested on exploration tasks. Geophysical FMs cover seismic data only, with no foundation model for gravity, magnetic, or electromagnetic methods. VLMs and agentic frameworks address

 doi:10.20944/preprints202607.2303.v1

adjacent geoscience tasks but have not been connected to exploration workflows. Concrete research opportunities arising from these gaps are discussed in Section 7.

6. Data Ecosystem and Tools

The availability of high-quality, accessible geoscientific data and robust software tools is fundamental to ML for mineral exploration. This section reviews the supporting ecosystem.

6.1. Datasets and Training Data

6.1.1. Global Datasets

Several global-scale datasets provide foundational information for mineral exploration ML:

- **USGS MRDS** [40]: The Mineral Resources Data System catalogues mineral deposit locations and characteristics, with the most thorough coverage for the United States and more limited records internationally. Systematic updates ceased in 2011, but it remains the most widely used global deposit database in MPM studies.
- **Global lithology maps:** The Global Lithological Map (GLiM) [163] provides polygon-based surface lithology classification assembled from geological maps at a target scale of 1:1,000,000, though the achieved resolution varies by region (area-weighted average approximately 1:3,750,000).
- **Geophysical grids:** The World Digital Magnetic Anomaly Map (WDMAM v2) [164] provides global magnetic anomaly coverage at 3 arc-minute resolution. Various global gravity models complement magnetic data at similar scales.
- **Crustal models:** CRUST1.0 [165] provides a global crustal model with 1-degree resolution, including sediment, crystalline crust, and Moho depth estimates.
- **Geochemical and mineral databases:** EarthChem [166] provides community-curated geochemical, geochronological, and petrological data, while OpenMindat [167] offers programmatic access to global mineral occurrence records.

An important limitation is that, with the exception of MRDS, these global datasets operate at resolutions far coarser than typical prospect-scale work (which requires 1:10,000–1:50,000 or better). They are therefore most useful for regional-scale screening and initial area reduction, not for direct targeting.

6.1.2. Purpose-Built Training Datasets

Several purpose-built datasets target specific ML tasks in geoscience:

- **SSL4EO-S12** [168]: A large-scale, globally sampled corpus of Sentinel-1/2 imagery for self-supervised pre-training of EO foundation models.
- **Noddyverse** [37]: One million synthetic 3D geological models with forward-modeled gravity and magnetic responses, enabling training for geological structure recovery and geophysical inversion without scarce real-world labels.
- **OpenEM** [169]: Large-scale multi-structural 3D datasets for electromagnetic methods, filling a critical gap in EM training data.
- **DARPA CriticalMAAS** [170]: Benchmark datasets for automated georeferencing and feature extraction from geological maps, organized by USGS and DARPA.

6.2. Data Portals

Geological surveys worldwide provide extensive geoscientific data through online portals. Table 5 summarizes the principal portals relevant to mineral exploration ML. National initiatives such as AusAEM [171] (continental airborne EM) and AusLAMP [172] (long-period magnetotellurics) in Australia demonstrate the scale of public geoscience data acquisition, while pan-regional platforms like EGDI aggregate data across national boundaries. In Africa, no unified data infrastructure comparable to EGDI currently exists, though individual national surveys are increasingly digitizing their holdings. A practical limitation is that most portals serve data through WMS/WFS or domain-specific file downloads, requiring substantial preprocessing before use as ML inputs.

 doi:10.20944/preprints202607.2303.v1

Table 5. Principal geoscience data portals relevant to mineral exploration ML, organized by region.

Region	Portal / Organization	URL	Key Data
Australia			
	Geoscience Australia [38]	https://portal.ga.gov.au/	National geology, geophysics, geochemistry
	SARIG (South Australia)	https://map.sarig.sa.gov.au/	Drillholes, geology, geophysics, tenements
	MinView (New South Wales)	https://minview.geoscience.nsw.gov.au/	500+ geoscience map layers
	GeoVIEW.WA (Western Australia)	https://geoview.dmp.wa.gov.au/geoview/	Geology, drillholes, geochemistry, tenements
	GeoVic (Victoria)	https://resources.vic.gov.au/geology-and-data/maps-reports-data/geovic	Geology, geophysics, mineral occurrences
	STRIKE (Northern Territory)	https://strike.nt.gov.au/	Geology, geophysics, geochemistry, drilling
	QLD Geoscience Data (Queensland)	https://geoscience.data.qld.gov.au/	Geology, geophysics, geochemistry, drilling
	MRT (Tasmania)	https://www.mrt.tas.gov.au/products/digital_data	Digital geological data
North America			
	USGS Mineral Resources	https://mrdata.usgs.gov/	Deposits, geochemistry, geophysics
	EarthExplorer (USGS)	https://earthexplorer.usgs.gov/	Satellite imagery, aerial photography
	GeologyOntario (Canada)	https://www.hub.geologyontario.mines.gov.on.ca/	Provincial geoscience data warehouse
	SIGEOM (Quebec, Canada)	https://sigeom.mines.gouv.qc.ca/	150+ years of geomining data
	MINFILE (British Columbia, Canada)	https://minfile.gov.bc.ca/	16,000+ mineral occurrences
South America			
	GeoSGB [173] (Brazil)	https://geosgb.sgb.gov.br/	Geology, geochemistry, geochronology, mineral occurrences
	GEOCATMIN (Peru)	https://geocatmin.ingemmet.gob.pe/	Geological maps, mining concessions
	SIGAM (Argentina)	https://sigam.segemar.gov.ar/	Geological and metallogenic maps
Europe			
	EGDI (pan-European)	https://www.europe-geology.eu/	Harmonized geology, mineral resources, geophysics
	BGS (United Kingdom)	https://www.bgs.ac.uk/	Geology, geophysics, geochemistry
	BRGM / Infoterre [174] (France)	https://infoterre.brgm.fr/	Subsurface data, geological maps
	GTK (Finland)	https://www.gtk.fi/en/	Bedrock geology, geochemistry, Hakku data service
	SGU (Sweden)	https://www.sgu.se/en/	Bedrock, geochemistry, groundwater
	NGU (Norway)	https://www.ngu.no/en	Geological maps, mineral resources, geophysics
Asia			
	NGAC (China)	http://www.ngac.org.cn/	National geological archives, mineral resources
	Bhukosh / GSI (India)	https://bhukosh.gsi.gov.in/Bhukosh/Public	147 geospatial layers, geophysics
Oceania			
	GNS Science (New Zealand)	https://data.gns.cri.nz/geology/	Geological maps, mineral occurrences
Africa			
	Council for Geoscience (South Africa)	https://www.geoscience.org.za/	Geology, geophysics, geochemistry

6.3. Software Frameworks and Tools

A growing ecosystem of open-source software supports ML workflows in mineral exploration. Table 6 summarizes the principal frameworks and tools.

 doi:10.20944/preprints202607.2303.v1

Table 6. Summary of major software frameworks and tools for ML-based mineral exploration, organized by category.

Framework / Tool	Primary Focus	Key Features	Category
Mineral Exploration Pipelines & Toolkits			
UNCOVER-ML [41]	Geoscience ML	Scalable ML pipeline; HPC/MPI support	Exploration pipeline
EIS Toolkit [175]	Prospectivity mapping	EU-funded; WoE, fuzzy overlay, spatial analysis	Exploration toolkit
GisSOM [176]	Geospatial data clustering	Geospatially-aware self-organizing maps	Exploration toolkit
Geoscience Domain Libraries			
GemPy [177]	3D geological modeling	Implicit modeling with uncertainty (stochastic)	Geological modeling
LoopStructural [178]	3D geological modeling	Implicit modeling; multiple interpolators	Geological modeling
Map2Loop [179]	3D model input generation	Automated constraint extraction from geological maps	Geological modeling
SimPEG [43]	Geophysical inversion	Modular simulation and parameter estimation	Geophysics
Fatiando a Terra [180]	Geophysics toolkit	Verde gridding, Boule ellipsoids, Harmonica	Geophysics
PyGIMLi [181]	Geophysical modeling & inversion	ERT, IP, seismics, gravimetry	Geophysics
Tomofast-x [182]	Geophysical inversion	Gravity/magnetic inversion; wavelet compression; HPC	Geophysics
dh2loop [183]	Drillhole data processing	Fuzzy-matching and thesaurus-based log standardization	Data processing
litho2strat [184]	Stratigraphic interpretation	Automated stratigraphy from drillhole lithological logs; UQ	Data processing
Data Infrastructure & Formats			
xarray [185]	N-D labeled arrays	Labeled dimensions; Dask parallel; NetCDF/Zarr I/O	Data infrastructure
rioxarray [186]	Geospatial raster operations	CRS-aware reprojection and clipping for xarray	Data infrastructure
Zarr [187]	Chunked N-D array storage	Chunked, compressed N-D arrays; parallel access	Data format
geoh5py [188]	Exploration data container	Drillholes, block models, surfaces; HDF5-based	Data format
Geospatial ML & Deep Learning Libraries			
TorchGeo [42]	Remote sensing DL	PyTorch datasets, samplers, transforms, pre-trained models	Deep learning
PySpatialML [189]	Raster ML	Scikit-learn compatible raster prediction	Raster ML
Terratorch [144]	FM fine-tuning	Fine-tune geospatial FMs (Prithvi, SatMAE, and others)	Deep learning
DKNN [190]	Interpolation	Deep kriging neural network	Geostatistics
General-Purpose Tools			
QGIS [191]	GIS	Free and open-source geographic information system	GIS
PyVista [192]	3D visualization	3D plotting and mesh analysis via VTK	Visualization
InterpretML [193]	Model interpretability	Glassbox and blackbox interpretability (EBMs, SHAP, LIME)	Explainability
SHAP [194]	Model interpretability	Unified feature attribution via Shapley values	Explainability

It illustrates that the open-source ecosystem spans the full ML workflow for mineral exploration, from data ingestion and geoscience-specific processing through to model training and interpretation. At the data layer, formats such as Zarr [187] and geoh5py [188] enable efficient handling of large, multi-dimensional exploration datasets, while libraries such as SimPEG [43] and GemPy [177] provide domain-specific modeling capabilities. For ML practitioners, TorchGeo [42] and Terratorch [144] offer PyTorch-native interfaces for remote sensing and foundation model fine-tuning, respectively. Explainability tools such as SHAP [194] and InterpretML [193] round out the pipeline by supporting model interpretation. As the table shows, the ecosystem is strongest for 2D raster workflows and geophysical inversion, while tooling for deep learning on irregular 3D data (drillholes, block models, unstructured meshes) is at its early stage.

7. Open Challenges and Research Opportunities

The ML methods reviewed in this paper share several challenges that cut across application domains. Rather than listing these as independent problems, we organize them by research maturity: challenges that current tools can address if adopted consistently (Section 7.1), near-term opportunities where methods from adjacent fields need domain-specific adaptation (Section 7.2), and long-term frontiers requiring fundamental research (Section 7.3).

7.1. Addressable with Current Methods

This subsection covers challenges where solutions exist but are not yet consistently adopted in mineral exploration ML.

Spatial validation.

Spatial cross-validation [8] is well-established in ecological modeling and geostatistics, yet many MPM studies still report results from random train/test splits that leak information through spatial autocorrelation [7]. Spatially-aware methods such as Spatial Random Forests [9] have demonstrated improved performance for subsurface applications. Adopting spatially blocked or leave-one-region-

Preprints.org (www.preprints.org) | NOT PEER-REVIEWED | Posted: 31 July 2026 doi:10.20944/preprints202607.2303.v1

out validation as a reporting standard would improve the reliability of published results without requiring new methodology.

Negative sample selection.

Most MPM studies generate negative training samples from random locations, which has been shown to introduce substantial variance in predictions [195]. More informative alternatives exist: barren drillholes, locations that have been physically tested and found to lack economic mineralization, provide a stronger training signal than random selection from unexplored terrain. Sensitivity analysis over different negative sampling strategies should become standard practice.

Data harmonization.

Geoscience data are collected across different time periods, organizations, methods, and standards, resulting in heterogeneous datasets requiring harmonization [10]. Common issues include inconsistent spatial resolution (e.g., 50 m geophysical grids vs. 1 km geochemical samples), compositional constraints in geochemical data [58], and legacy data in non-standardized formats. The scale of this challenge is substantial. For instance, the Western Australian drillhole database alone contains over 2 million holes from more than 1,500 companies, each using proprietary lithological codes and logging conventions [183], while Australian geological surveys collectively hold over 5 million drillhole logs, most lacking standardized stratigraphic assignments [184]. Developing universal lithological ontologies and automated harmonization methods is a prerequisite for continent-scale ML applications. Tools such as dh2loop [183] (NLP-based fuzzy matching for drillhole log standardization) and litho2strat [184] (stratigraphic sequence recovery with uncertainty quantification) demonstrate that automated harmonization is becoming viable and should be integrated into standard preprocessing workflows. Underpinning such efforts is the need for comprehensive geological ontologies that provide formal, machine-readable definitions of geological concepts. The GeoCore ontology [196] defines a core set of geological concepts (objects, materials, boundaries, structures, processes) grounded in formal ontological principles, providing a shared semantic backbone for integrating knowledge across geological sub-fields. The GeoScience Ontology (GSO) [39], developed as part of the Loop3D project, complements this by offering a modular, OWL-based framework for representing geological types and relationships, enabling cross-domain and multilingual harmonization of geoscience data. Broader adoption of such ontologies would provide the semantic foundation needed for continent-scale, multi-source ML applications.

Benchmarks.

Geoscience ML lacks equivalents to ImageNet or GLUE for mineral exploration tasks. Community-accepted benchmark suites with defined evidence layers, spatially-aware train/test splits, shared evaluation metrics, and transparent reporting of preprocessing and hyperparameters would accelerate progress and enable meaningful cross-study comparison.

7.2. Near-Term Research Opportunities

This subsection covers challenges where methods exist in the broader ML literature but require domain-specific adaptation for mineral exploration.

Uncertainty quantification.

Three distinct sources of uncertainty arise in MPM and are often conflated: **(i)** label uncertainty, stemming from the PU nature of the problem where absence of a known deposit does not confirm absence of mineralization; **(ii)** input-data uncertainty, from measurement errors, interpolation artifacts, and inconsistent data quality across surveys; and **(iii)** model uncertainty, reflecting both epistemic uncertainty (reducible with more data) and aleatoric uncertainty (irreducible noise) [197]. Bayesian neural networks [198], ensemble methods, Monte Carlo dropout [199], and conformal prediction [200] each address different aspects of this decomposition but need calibration for geoscience settings where

 doi:10.20944/preprints202607.2303.v1

spatial correlation violates the exchangeability assumptions of standard conformal methods [66]. Bayesian deep learning for MPM [90] has demonstrated that calibrated uncertainty maps can distinguish areas of genuinely low prospectivity from areas where predictions are unreliable due to data sparsity, directly informing exploration investment decisions.

Explainability beyond feature attribution.

Post-hoc methods such as SHAP [194] provide per-feature importance scores but do not validate whether model reasoning aligns with established geological knowledge [193]. A more rigorous approach would test model explanations against domain constraints: for example, if a model identifies a geochemical feature as important for a porphyry copper prediction, does this align with known alteration geochemistry for that deposit type? Developing geologically-grounded evaluation of model explanations, rather than treating explanation as a purely statistical exercise, is an open opportunity.

Cross-terrane transfer learning.

Transfer learning has been applied to address data scarcity in MPM, for example by pre-training on geological classification tasks within a study area [23]. However, cross-region transfer remains largely untested. We note that success is likely to depend on geological compatibility between source and target regions: transfer may succeed when regions share similar deposit types, tectonic settings, and evidence-layer definitions, but may fail when the same geophysical or geochemical signature has different geological meaning in different terranes (fault-bounded crustal blocks, each with a distinct geological history). Domain adaptation methods that explicitly model which features are transferable and which are region-specific represent a promising direction. Characterizing geological similarity between terranes as a prerequisite for transfer, rather than treating it purely as an ML domain adaptation problem, would ground these methods in geological reality.

Positive-Unlabeled learning.

The PU nature of mineral exploration data [6] means that standard classification metrics (accuracy, F1) are unreliable because the ground truth is incomplete. Known mineral deposits are extremely rare relative to study area size, with typical class ratios of 1:10,000 or worse, and the absence of a known deposit does not confirm absence of mineralization. PU bagging [201], synthetic augmentation [21,202], and semi-supervised learning [109] partially address this, but the field lacks consensus on how positives are defined (individual deposits vs. mineral occurrences vs. geochemical anomalies), how unlabeled samples are selected, and whether sensitivity analysis under different assumptions about the unlabeled regions should be mandatory. Developing evaluation protocols specifically designed for PU geospatial settings is an open need.

Active learning for exploration.

Active learning [203] offers a principled response to label scarcity: iteratively selecting the most informative locations for sampling or drilling to maximize information gain while reducing exploration cost. Bayesian optimization provides a principled framework for this sequential decision-making: Haan et al. [204] demonstrated multi-objective Bayesian optimization with Gaussian Process surrogates for joint geophysical inversion and optimal drill-core placement, balancing exploration and exploitation through acquisition functions applied to gravity and magnetic data. Coupling active learning with uncertainty quantification is a natural synergy, as model uncertainty directly informs where additional data would be most valuable.

7.3. Long-Term Research Frontiers

This subsection covers challenges that require fundamental research and are unlikely to be fully resolved with existing methods.

 doi:10.20944/preprints202607.2303.v1

Multi-modal foundation models.

Current geoscience foundation models are largely modality-specific (Section 5): EO models process satellite imagery, seismic models handle reflection data, and LLMs reason over text. No single model spans the full range of exploration data (geophysical grids, geochemical assays, geological maps, remote sensing, text). Building multi-modal models that jointly encode these heterogeneous inputs is a fundamental research challenge due to their different spatial samplings, physical units, and information content. Terramind [128] represents an early step for EO modalities, but extending this to include tabular geochemistry or irregular geophysical surveys requires new architectural approaches for handling mixed regular and irregular spatial data.

3D and 4D spatiotemporal modeling.

Extending ML-based prospectivity from 2D surface prediction to 3D subsurface models remains a significant challenge [65]. Most deposits lie at depth, yet the majority of MPM methods operate on 2D surface projections of evidence layers. Implicit neural representations can model continuous 3D geological properties from sparse borehole observations, but scaling these to regional extents with uncertainty quantification is unresolved. Incorporating geological time adds a further dimension: plate tectonic reconstruction frameworks [54] provide the temporal context needed to assess whether favorable conditions existed at the right time in a region's history, but integrating these with ML-based prospectivity is largely unexplored. Topological representations that encode spatial and temporal adjacency between geological units [205], capturing contact relationships and relative chronological ordering, are a natural fit for GNN architectures but have not been applied to prospectivity modeling. A further gap is encoding post-formation preservation: as widely recognized in mineral systems thinking, a deposit must not only form (requiring appropriate source, pathway, and trap) but also survive subsequent geological processes such as erosion or deep burial, yet preservation potential is rarely incorporated as an ML feature or constraint.

Agentic AI for exploration workflows.

AI agents that autonomously orchestrate multi-step exploration workflows, querying databases, invoking domain-specific models, and synthesizing evidence across modalities (Section 5.5), represent a frontier beyond current static inference pipelines. For mineral exploration, an agentic system could iteratively refine targeting by selecting which data to acquire next, which models to run, and how to combine their outputs. This requires not only robust foundation models for each modality but also reliable uncertainty communication between components and the ability to reason about the geological plausibility of intermediate results.

Real-time adaptive exploration.

Modern exploration increasingly generates continuous data streams from downhole logging tools, drone-mounted sensors, and real-time geochemical analyzers. ML systems that ingest streaming data and update prospectivity models incrementally (online learning rather than batch retraining) could enable adaptive campaigns that redirect field activities based on incoming results. This requires solutions for edge computing in remote field deployments, continual learning without catastrophic forgetting, and real-time uncertainty updating.

Ethical and environmental considerations.

As ML guides exploration targeting, several considerations warrant attention: the environmental impact of AI-directed exploration activity, transparency in AI-assisted regulatory decisions, responsible handling of indigenous cultural heritage data in training sets, and equitable distribution of extraction benefits. The carbon footprint of training large foundation models should also be weighed against potential efficiency gains from reducing unnecessary exploration activity. Intellectual property and data ownership pose further challenges, as proprietary drill-hole logs and geochemical assays often carry restrictive licensing, creating tension between ML data requirements and the rights of data

 doi:10.20944/preprints202607.2303.v1

originators; clear ownership and fair-use frameworks for public versus privately funded exploration data remain an open policy question.

8. Conclusions

This survey has reviewed ML and foundation models for mineral exploration, from domain-specific methods that produce geological, geophysical, geochemical, and remote sensing evidence layers, through MPM that integrates these layers for targeting, to foundation models and NLP tools that introduce transfer learning and text-derived knowledge into exploration workflows. MPM remains the most mature ML application, now spanning ensemble methods, deep learning, and self-supervised paradigms. Foundation models exist for EO imagery, seismic data, and geoscience text individually, but only the text-to-prospectivity pathway has demonstrated end-to-end integration with mineral exploration. Persistent challenges, including spatial non-stationarity, label scarcity, data heterogeneity, and uncertainty quantification, require domain-aware solutions rather than off-the-shelf ML approaches.

The most impactful near-term opportunities lie in connecting these modality-specific building blocks: multi-modal foundation models that jointly reason across imagery, geophysics, geochemistry, and text, and AI agents that autonomously orchestrate exploration workflows across these data types. Realizing this vision will require standardized benchmarks, spatially-aware evaluation protocols, and closer collaboration between the ML and geoscience communities.

Acknowledgments: The authors acknowledge the University of Western Australia for providing a PhD scholarship supporting this research. This work was supported by the Australian Research Council (ARC) Discovery Grants DP260101891 and DP220102197, and Future Fellowship FT250100448. The authors also thank the mineral exploration machine learning community for maintaining the open-source repository of resources that informed this survey.

References

1. International Energy Agency. The Role of Critical Minerals in Clean Energy Transitions. Technical report, IEA, Paris, 2021. Licence: CC BY 4.0.
2. Hronsky, J.M.A.; Groves, D.I. Science of targeting: definition, strategies, targeting and performance measurement. *Australian Journal of Earth Sciences* **2008**, *55*, 3–12. https://doi.org/10.1080/08120090701581356.
3. Dentith, M.; Mudge, S.T. *Geophysics for the Mineral Exploration Geoscientist*; Cambridge University Press, 2014. https://doi.org/10.1017/CBO9781139024358.
4. Bonham-Carter, G.F. *Geographic Information Systems for Geoscientists: Modelling with GIS*; Pergamon Press: Oxford, 1994.
5. Bergen, K.J.; Johnson, P.A.; de Hoop, M.V.; Beroza, G.C. Machine learning for data-driven discovery in solid Earth geoscience. *Science* **2019**, *363*, eaau0323. https://doi.org/10.1126/science.aau0323.
6. Bekker, J.; Davis, J. Learning from Positive and Unlabeled Data: A Survey. *Machine Learning* **2020**, *109*, 719–760. https://doi.org/10.1007/s10994-020-05877-5.
7. Tobler, W.R. A computer movie simulating urban growth in the Detroit region. *Economic Geography* **1970**, *46*, 234–240. https://doi.org/10.2307/143141.
8. Roberts, D.R.; Bahn, V.; Ciuti, S.; Boyce, M.S.; Elith, J.; Guillera-Arroita, G.; Hauenstein, S.; Lahoz-Monfort, J.J.; Schröder, B.; Thuiller, W.; et al. Cross-validation strategies for data with temporal, spatial, hierarchical, or phylogenetic structure. *Ecography* **2017**, *40*, 913–929. https://doi.org/10.1111/ecog.02881.
9. Merzoug, A.; Özbayrak, F.; Foster, J.T.; Pyrcz, M.J. Beyond random forest: how spatial bagging and spatial random forest dominate for subsurface applications? *Computational Geosciences* **2025**.
10. Data Quality Contributors. Geoscience Data Quality for Machine Learning. https://github.com/RichardScottOZ/Geoscience-Data-Quality-for-Machine-Learning, 2023.
11. Silva dos Santos, V.; Gloaguen, E.; Tirdad, S. Lithological mapping using Spatially Constrained Bayesian Network. *Computers & Geosciences* **2025**.
12. Yang, F.; Zuo, R.; Kreuzer, O.P. Interpretable regional-scale geological mapping using a contrastive graph attention network for multimodal data fusion and recognition of controlling factors. *Engineering Geology* **2026**, *361*, 108508. https://doi.org/10.1016/j.enggeo.2025.108508.

 doi:10.20944/preprints202607.2303.v1

13. Raissi, M.; Perdikaris, P.; Karniadakis, G.E. Physics-informed neural networks: A deep learning framework for solving forward and inverse problems involving nonlinear partial differential equations. *Journal of Computational Physics* **2019**, *378*, 686–707. https://doi.org/10.1016/j.jcp.2018.10.045.
14. bin Waheed, U.; Alkhalifah, T.; Haghighat, E.; Song, C.; Virieux, J. Seismic tomography using physics-informed neural networks. *arXiv preprint arXiv:2104.01588* **2021**.
15. Soltani, Z.; Hassani, H.; Esmaeiloghli, S. A deep autoencoder network connected to geographical random forest for spatially aware geochemical anomaly detection. *Computers & Geosciences* **2024**, *190*, 105657. https://doi.org/10.1016/j.cageo.2024.105657.
16. Farahbakhsh, E.; Goel, D.; Pimparkar, D.; Müller, R.D.; Chandra, R. Convolutional Neural Networks for Mineral Prospecting Through Alteration Mapping with Remote Sensing Data. *PFG – Journal of Photogrammetry, Remote Sensing and Geoinformation Science* **2025**, *93*, 379–400. https://doi.org/10.1007/s41064-025-00344-z.
17. Feng, X.; Huang, J.; Chen, X.; Zhou, H.; Zhang, M.; Zhang, C.; Ye, F. Research on hyperspectral remote sensing alteration mineral mapping using an improved ViT model. *Computers & Geosciences* **2026**, *206*, 106037. https://doi.org/10.1016/j.cageo.2025.106037.
18. Bonham-Carter, G.F.; Agterberg, F.P.; Wright, D.F. Weights of evidence modelling: a new approach to mapping mineral potential. In *Statistical Applications in the Earth Sciences*; Agterberg, F.P.; Bonham-Carter, G.F., Eds.; Geological Survey of Canada, 1989; pp. 171–183. Paper 89-9.
19. Breiman, L. Random Forests. *Machine Learning* **2001**, *45*, 5–32. https://doi.org/10.1023/A:1010933404324.
20. Goodfellow, I.; Pouget-Abadie, J.; Mirza, M.; Xu, B.; Warde-Farley, D.; Ozair, S.; Courville, A.; Bengio, Y. Generative adversarial nets. In Proceedings of the Adv. Neural Inform. Process. Syst., 2014, pp. 2672–2680.
21. Wake, N.; Farahbakhsh, E.; Muller, R.D. Lateritic Ni-Co prospectivity modeling in eastern Australia using an enhanced generative adversarial network and positive-unlabeled bagging. *Natural Resources Research* **2024**. Data at https://zenodo.org/records/14037494.
22. Farahbakhsh, E.; Maughan, J.; Muller, R.D. Critical mineral prospectivity mapping on the Gawler craton using a new machine learning framework. In Proceedings of the 4th Australasian Exploration Geoscience Conference (AEGC), Brisbane, Australia, 2023. https://github.com/e-farahbakhsh/Gawler_MPM.
23. Mantilla-Dulcey, A.; Goyes-Penafiel, P.; Baez-Rodriguez, R.; Khurama, S. Porphyry-type mineral prospectivity mapping with imbalanced data via prior geological transfer learning. *Gondwana Research* **2024**, *136*, 236–250. https://github.com/Anagabrielamantilla/TransferProspectivityLearning, https://doi.org/10.1016/j.gr.2024.09.004.
24. Li, X.; Zhao, C.; Yuan, F.; Li, Y.; Zheng, C.; Zhang, M.; Ge, C.; Guo, D.; Lan, X.; Lu, S. 3D GCN–CNN Hybrid Model for 3D Mineral Prospectivity Modeling of Porphyry- and Skarn-Type Mineralization. *Natural Resources Research* **2025**. https://doi.org/10.1007/s11053-025-10593-9.
25. Bommasani, R.; Hudson, D.A.; Adeli, E.; Altman, R.; Arber, S.; von Arx, S.; Bernstein, M.S.; Bohg, J.; Bosselut, A.; Brunskill, E.; et al. On the Opportunities and Risks of Foundation Models. *arXiv preprint arXiv:2108.07258* **2021**.
26. Clay Foundation. Clay: An Open Source AI Model and Interface for Earth. https://github.com/Clay-foundation/model, 2024.
27. IBM.; NASA. Prithvi: IBM-NASA Geospatial Foundation Model. https://huggingface.co/ibm-nasa-geospatial, 2024.
28. Sheng, H.; Wu, X.; Si, X.; Li, J.; Zhang, S.; Duan, X. Seismic Foundation Model: A new generation deep learning model in geophysics. https://github.com/shenghanlin/SeismicFoundationModel, 2023.
29. Dou, Y.; Wu, X.; Bangs, N.L.; Sethi, H.S.; Li, J.; Gao, H.; Guo, Z. Geological Everything Model 3D: A Physics-informed Promptable Foundation Model for Unified and Zero-Shot Subsurface Understanding. *arXiv preprint arXiv:2507.00419* **2025**.
30. Deng, C.; Zhang, T.; He, Z.; Xu, Y.; Chen, Q.; Shi, Y.; Fu, L.; Zhang, W.; Wang, X.; Zhou, C.; et al. Learning Foundation Language Models for Geoscience Knowledge Understanding and Utilization. *arXiv preprint arXiv:2306.05064* **2023**.
31. Lin, Z.; Deng, C.; Zhou, L.; Zhang, T.; Xu, Y.; Xu, Y.; He, Z.; Shi, Y.; Dai, B.; Song, Y.; et al. GeoGalactica: A Larger Foundation Language Model in Geoscience. *arXiv preprint arXiv:2401.00434* **2024**.
32. Chen, Z.; Lin, M.; Zang, M.; Wang, Z.; Li, J.; Bai, Y. JiuZhou: Open Foundation Language Models for Geoscience. *International Journal of Digital Earth* **2025**. https://doi.org/10.1080/17538947.2025.2449708.
33. Padarian, J.; Fuentes, I. GeoVec: Word embedding model trained on geoscience papers. *SOIL* **2019**, *5*, 177–187.

 doi:10.20944/preprints202607.2303.v1

34. Liu, H.; Qiu, Q.; Wu, L.; Li, W.; Wang, B.; Zhou, Y. Few-shot learning for name entity recognition in geological text based on GeoBERT. *Earth Science Informatics* **2022**, *15*, 979–991. https://doi.org/10.1007/s12145-022-00775-x.
35. Li, W.; Ma, X.; Wang, X.; Wu, L.; Salati, S.; Xie, Z. Stratigraphic Knowledge Graph (StraKG). *Applied Computing and Geosciences* **2024**.
36. Lawley, C.J.; Gadd, M.G.; Parsa, M.; Lederer, G.W.; Graham, G.E.; Ford, A. Applications of Natural Language Processing to Geoscience Text Data and Prospectivity Modeling. *Natural Resources Research* **2023**. https://doi.org/10.1007/s11053-023-10216-1.
37. Jessell, M.; Guo, J.; Li, Y.; Lindsay, M.; Scalzo, R.; Giraud, J.; Pirot, G.; Cripps, E.; Ogarko, V. Into the Noddyverse: a massive data store of 3D geological models for machine learning and inversion applications. *Earth System Science Data* **2022**, *14*, 381–392. https://doi.org/10.5194/essd-14-381-2022.
38. Geoscience Australia. Geoscience Australia Data Portal. https://portal.ga.gov.au/, 2024.
39. Brodaric, B.; Richard, S.M. The GeoScience Ontology reference. Open File 8796, Geological Survey of Canada, 2021. https://doi.org/10.4095/328296.
40. U.S. Geological Survey. USGS Mineral Resources Data System (MRDS). https://mrdata.usgs.gov/mrds/, 2024.
41. Geoscience Australia. Uncover-ML: A machine learning framework for geoscience prospectivity mapping. https://github.com/GeoscienceAustralia/uncover-ml, 2020.
42. Microsoft. TorchGeo: datasets, samplers, transforms, and pre-trained models for geospatial data. https://github.com/microsoft/torchgeo, 2022.
43. SimPEG Authors. SimPEG: Simulation and Parameter Estimation in Geophysics. https://github.com/simpeg/simpeg, 2015.
44. Bergen, K.J.; Johnson, P.A.; de Hoop, M.V.; Beroza, G.C. Machine learning for data-driven discovery in solid Earth geoscience. *Science* **2019**, *363*, eaau0323, [https://www.science.org/doi/pdf/10.1126/science.aau0323]. https://doi.org/10.1126/science.aau0323.
45. Zuo, R.; Xiong, Y.; Wang, J.; Carranza, E.J.M. Deep learning and its application in geochemical mapping. *Earth-Science Reviews* **2019**, *192*, 1–14. https://doi.org/https://doi.org/10.1016/j.earscirev.2019.02.023.
46. Dramsch, J.S. Chapter One - 70 years of machine learning in geoscience in review. In *Machine Learning in Geosciences*; Moseley, B.; Krischer, L., Eds.; Elsevier, 2020; Vol. 61, *Advances in Geophysics*, pp. 1–55. https://doi.org/https://doi.org/10.1016/bs.agph.2020.08.002.
47. Zuo, R. Geodata Science-Based Mineral Prospectivity Mapping: A Review. *Natural Resources Research* **2020**, *29*, 3415–3424. https://doi.org/10.1007/s11053-020-09700-9.
48. Zuo, R.; Kreuzer, O.P.; Wang, J.; Xiong, Y.; Zhang, Z.; Wang, Z. Uncertainties in GIS-Based Mineral Prospectivity Mapping: Key Types, Potential Impacts and Possible Solutions. *Natural Resources Research* **2021**, *30*, 3059–3079. https://doi.org/10.1007/s11053-021-09871-z.
49. Sun, K.; Chen, Y.; Geng, G.; Lu, Z.; Zhang, W.; Song, Z.; Guan, J.; Zhao, Y.; Zhang, Z. A Review of Mineral Prospectivity Mapping Using Deep Learning. *Minerals* **2024**, *14*, 1021. https://doi.org/10.3390/min14101021.
50. Yang, F.; Zuo, R.; Kreuzer, O.P. Artificial intelligence for mineral exploration: A review and perspectives on future directions from data science. *Earth-Science Reviews* **2024**, *258*, 104941. https://doi.org/https://doi.org/10.1016/j.earscirev.2024.104941.
51. Fu, Z.; Zheng, X.; Yan, Y.; Xu, X.; Zhou, F.; Li, X.; Zhou, Q.; Mai, W. The Evolution of Machine Learning in Large-Scale Mineral Prospectivity Prediction: A Decade of Innovation (2016–2025). *Minerals* **2025**, *15*, 1042. https://doi.org/10.3390/min15101042.
52. Zhang, H.; Xu, J.J.; Cui, H.W.; Li, L.; Yang, Y.; Tang, C.S.; Boers, N. When Geoscience Meets Foundation Models: Toward a general geoscience artificial intelligence system. *IEEE Geoscience and Remote Sensing Magazine* **2025**, *13*, 79–118. https://doi.org/10.1109/MGRS.2024.3496478.
53. Carranza, E.J.M. *Geochemical Anomaly and Mineral Prospectivity Mapping in GIS*; Vol. 11, *Handbook of Exploration and Environmental Geochemistry*, Elsevier: Amsterdam, 2009.
54. Boone, S.C.; Glorie, S.; Zahirovic, S.; Nixon, A.; Meeuws, F.; Kohlmann, F. Deciphering mantle, tectonic and climatic drivers of exhumation. *Communications Earth & Environment* **2025**. https://doi.org/10.1038/s43247-025-03005-6.
55. Zhou, J.; Farahbakhsh, E.; Williams, S.; Li, X.; Liu, Y.; Li, S.; Muller, R.D. Machine Learning and Big Data Mining Reveal Earth's Deep Time Crustal Thickness and Tectonic Evolution: A New Chemical Mohometry

Approach. *Journal of Geophysical Research: Solid Earth* **2025**, *130*, e2024JB030404. https://doi.org/10.1029/2024JB030404.
56. Rose, A.W.; Hawkes, H.E.; Webb, J.S. *Geochemistry in Mineral Exploration*, 2nd ed.; Academic Press: New York, 1979.
57. McClenaghan, M.B. Indicator mineral methods in mineral exploration. *Geochemistry: Exploration, Environment, Analysis* **2005**, *5*, 233–245. https://doi.org/10.1144/1467-7873/03-066.
58. Aitchison, J. The Statistical Analysis of Compositional Data. *Journal of the Royal Statistical Society. Series B (Methodological)* **1982**, *44*, 139–177.
59. Sabins, F.F. Remote sensing for mineral exploration. *Ore Geology Reviews* **1999**, *14*, 157–183. https://doi.org/10.1016/S0169-1368(99)00007-4.
60. Dimeski, A.; Rahimi, A. Automated Extraction of Mining Company Drillhole Results. In Proceedings of the Proceedings of W-NUT 2022, 2022. https://aclanthology.org/2022.wnut-1.16/.
61. Dong, J.; Qiu, Q.; Xie, Z.; Ma, K.; Hu, A.; Wang, H. Understanding table content for mineral exploration reports using deep learning and natural language processing. *Ore Geology Reviews* **2023**.
62. Dawson, H.L.; Dubrule, O.; John, C.M. Impact of dataset size and convolutional neural network architecture on transfer learning for carbonate rock classification. *Computers & Geosciences* **2023**, *171*, 105284. https://doi.org/10.1016/j.cageo.2022.105284.
63. Chen, Z.; Zheng, C.; Zhang, M.; Hu, Z.; Duan, J. PetroMind: A multimodal petrographic model for rock image classification and lithological description generation. *Applied Computing and Geosciences* **2026**, *29*, 100314. https://doi.org/https://doi.org/10.1016/j.acags.2025.100314.
64. Fu, D.; Su, C.; Wang, W.; Yuan, R. Deep learning based lithology classification of drill core images. *PLoS ONE* **2022**, *17*, e0270826. https://doi.org/10.1371/journal.pone.0270826.
65. Hillier, M.; Wellmann, F.; de Kemp, E.A.; Brodaric, B.; Schetselaar, E.; Bédard, K. GeoINR 1.0: an implicit neural network approach to three-dimensional geological modelling. *Geoscientific Model Development* **2023**, *16*, 6987–7012. https://doi.org/10.5194/gmd-16-6987-2023.
66. Gao, K.; Hillier, M.; Wellmann, F. Uncertainty quantification using Hamiltonian Monte Carlo for structural geological modelling with implicit neural representations. *Computers & Geosciences* **2026**, *209*.
67. Jiang, Z.; Mallants, D.; Gao, L.; Munday, T.; Mariethoz, G.; Peeters, L. Sub3DNet1.0: a deep-learning model for regional-scale 3D subsurface structure mapping. *Geoscientific Model Development* **2021**, *14*, 3421–3435.
68. Ghyselincks, S.; Okhmak, V.; Zampini, S.; Turkiyyah, G.; Keyes, D.; Haber, E. Synthetic Geology: Structural Geology Meets Deep Learning. *arXiv preprint arXiv:2506.11164* **2025**.
69. Lipman, Y.; Chen, R.T.Q.; Ben-Hamu, H.; Nickel, M.; Le, M. Flow Matching for Generative Modeling. In Proceedings of the The Eleventh International Conference on Learning Representations, 2023.
70. Pawley, S.M.; Atkinson, L.; Utting, D.J.; Hartman, G.M.D.; Atkinson, N. Evaluating spatially enabled machine learning approaches for depth to bedrock mapping. *PLOS ONE* **2024**. https://doi.org/10.1371/journal.pone.0296881.
71. He, S.; Cai, H.; Liu, S.; Xie, J.; Hu, X. Recovering 3D Basement Relief Using Gravity Data Through Convolutional Neural Networks. *Journal of Geophysical Research: Solid Earth* **2021**, *126*, e2021JB022611. https://doi.org/10.1029/2021JB022611.
72. Guo, J.; Li, Y.; Jessell, M.W.; Giraud, J.; Li, C.; Wu, L.; Li, F.; Liu, S. 3D geological structure inversion from Noddy-generated magnetic data using deep learning methods. *Computers & Geosciences* **2021**, *149*, 104701. https://doi.org/https://doi.org/10.1016/j.cageo.2021.104701.
73. Bavandsavadkoohi, M.; Cedou, M.; Blouin, M.; Gloaguen, E.; Tirdad, S.; Giroux, B. High-resolution aeromagnetic map through Adapted-SRGAN. *Computers & Geosciences* **2023**.
74. Saibi, H.; Hireche, A.; Tsuji, T.; Ali, M.Y.; Ahmad, A.B. Comparison of Deep Learning Models for 1D Magnetotelluric Inversion. *Applied Computing and Geosciences* **2026**, *29*, 100320. https://doi.org/10.1016/j.acags.2026.100320.
75. Davis, W.J.S.; et al. Using NeuralOperator for Geophysical Surrogate Modeling. https://github.com/williamjsdavis/GP-cubed, 2026.
76. Yang, Y.; Gao, A.F.; Castellanos, J.C.; Ross, Z.E.; Azizzadenesheli, K.; Clayton, R.W. Seismic wave propagation and inversion with neural operators. *The Seismic Record* **2021**, *1*, 126–134. https://doi.org/10.1785/0320210026.
77. Li, Z.; Kovachki, N.; Azizzadenesheli, K.; Liu, B.; Bhattacharya, K.; Stuart, A.; Anandkumar, A. Fourier Neural Operator for Parametric Partial Differential Equations. In Proceedings of the International Conference on Learning Representations, 2021.

 doi:10.20944/preprints202607.2303.v1

78. Georganos, S.; Grippa, T.; Gadiaga, A.N.; Linard, C.; Lennert, M.; Vanhuysse, S.; Mboga, N.; Wolff, É.; Kalogirou, S. Geographical random forests: a spatial extension of the random forest algorithm to address spatial heterogeneity in remote sensing and population modelling. *Geocarto International* **2021**, *36*, 121–136. https://doi.org/10.1080/10106049.2019.1595177.
79. Pang, G.; Shen, C.; van den Hengel, A. Deep Anomaly Detection with Deviation Networks. In Proceedings of the Proceedings of the 25th ACM SIGKDD International Conference on Knowledge Discovery and Data Mining (KDD), 2019, pp. 353–362. https://doi.org/10.1145/3292500.3330871.
80. Luo, Z.; Farahbakhsh, E.; Muller, R.D.; Zuo, R. Multivariate statistical analysis and bespoke deviation network modeling for geochemical anomaly detection of rare earth elements. *Applied Geochemistry* **2024**.
81. Carrasco-Godoy, C.; Campbell, I.H.; Cajal, Y. Quantifying the Criteria Used to Identify Zircons from Ore-Bearing and Barren Systems in Porphyry Copper Exploration. *Economic Geology* **2024**, *119*, 1035–1058. https://doi.org/10.5382/econgeo.5086.
82. Wen, Z.H.; Xu, B.; Kirkland, C.L.; Lentz, D.R.; Hou, Z.Q.; Wang, T.; Yuan, M.W. Machine Learning Zircon Trace Element Tool to Predict Porphyry Deposit Type and Resource Size. *Journal of Geophysical Research: Machine Learning and Computation* **2024**. https://doi.org/10.1029/2024JH000180.
83. Wen, Z.H.; Li, L.; Kirkland, C.L.; Li, S.R.; Sun, X.J.; Lei, J.L.; Xu, B.; Hou, Z.Q. A machine learning approach to discrimination of igneous rocks and ore deposits by zircon trace elements. *American Mineralogist* **2024**, *109*, 1129–1142. https://doi.org/10.2138/am-2022-8899.
84. Ágreda-López, M.; Parodi, V.; Musu, A.; Jorgenson, C.; Carfì, A.; Mastrogiovanni, F.; Caricchi, L.; Perugini, D.; Petrelli, M. Enhancing machine learning thermobarometry for clinopyroxene-bearing magmas. *Computers & Geosciences* **2024**, *193*, 105707.
85. Clark, R.N. Spectroscopy of Rocks and Minerals, and Principles of Spectroscopy. In *Manual of Remote Sensing, Volume 3: Remote Sensing for the Earth Sciences*; Rencz, A.N., Ed.; John Wiley & Sons, 1999; pp. 3–58.
86. Bioucas-Dias, J.M.; Plaza, A.; Dobigeon, N.; Parente, M.; Du, Q.; Gader, P.; Chanussot, J. Hyperspectral Unmixing Overview: Geometrical, Statistical, and Sparse Regression-Based Approaches. *IEEE Journal of Selected Topics in Applied Earth Observations and Remote Sensing* **2012**, *5*, 354–379. https://doi.org/10.1109/JSTARS.2012.2194696.
87. Gao, Y.; Pan, B.; Xu, X.; Song, X.; Shi, Z. A Reversible Generative Network for Hyperspectral Unmixing with Spectral Variability. *IEEE Transactions on Geoscience and Remote Sensing* **2024**. https://doi.org/10.1109/TGRS.2024.3536904.
88. Kirillov, A.; Mintun, E.; Ravi, N.; Mao, H.; Rolland, C.; Gustafson, L.; Xiao, T.; Whitehead, S.; Berg, A.C.; Lo, W.Y.; et al. Segment Anything. In Proceedings of the Proceedings of the IEEE/CVF International Conference on Computer Vision (ICCV), 2023, pp. 4015–4026.
89. OpenGeos. Segment-geospatial: Segment Anything for Geospatial Uses. https://github.com/opengeos/segment-geospatial, 2024.
90. Liu, Y. Quantifying uncertainty of mineral prediction using a novel Bayesian deep learning framework. *Artificial Intelligence in Geosciences* **2025**.
91. Cortes, C.; Vapnik, V. Support-vector networks. *Machine Learning* **1995**, *20*, 273–297. https://doi.org/10.1007/BF00994018.
92. Zuo, R.; Carranza, E.J.M. Support vector machine: A tool for mapping mineral prospectivity. *Computers & Geosciences* **2011**, *37*, 1967–1975. https://doi.org/10.1016/j.cageo.2010.09.014.
93. Chen, T.; Guestrin, C. XGBoost: A Scalable Tree Boosting System. In Proceedings of the Proceedings of the 22nd ACM SIGKDD International Conference on Knowledge Discovery and Data Mining, 2016, pp. 785–794. https://doi.org/10.1145/2939672.2939785.
94. Ke, G.; Meng, Q.; Finley, T.; Wang, T.; Chen, W.; Ma, W.; Ye, Q.; Liu, T.Y. LightGBM: A Highly Efficient Gradient Boosting Decision Tree. In Proceedings of the Adv. Neural Inform. Process. Syst., 2017, pp. 3149–3157.
95. Yin, B.; Zuo, R.; Xiong, Y. Mineral Prospectivity Mapping via Gated Recurrent Unit Model. *Natural Resources Research* **2022**, *31*, 2065–2079. https://doi.org/10.1007/s11053-021-09979-2.
96. Yin, B.; Zuo, R.; Sun, S. Mineral Prospectivity Mapping Using Deep Self-Attention Model. *Natural Resources Research* **2023**, *32*, 37–56. https://doi.org/10.1007/s11053-022-10142-8.
97. Yang, F.; Zuo, R. Geologically Constrained Convolutional Neural Network for Mineral Prospectivity Mapping. *Mathematical Geosciences* **2024**, *56*, 1605–1628. https://doi.org/10.1007/s11004-024-10141-w.
98. Zuo, R.; Xu, Y. Graph Deep Learning Model for Mapping Mineral Prospectivity. *Mathematical Geosciences* **2023**, *55*, 1–21. https://doi.org/10.1007/s11004-022-10015-z.

 doi:10.20944/preprints202607.2303.v1

99. Xu, Y.; Zuo, R. An Interpretable Graph Attention Network for Mineral Prospectivity Mapping. *Mathematical Geosciences* **2024**, *56*, 169–190. https://doi.org/10.1007/s11004-023-10076-8.
100. Li, C.; Xiao, K.; Sun, L.; Tang, R.; Dong, X.; Qiao, B.; Xu, D. CNN-Transformers for mineral prospectivity mapping in the Maodeng–Baiyinchagan area, Southern Great Xing'an Range. *Ore Geology Reviews* **2024**, *167*, 106007. https://doi.org/10.1016/j.oregeorev.2024.106007.
101. Vaswani, A.; Shazeer, N.; Parmar, N.; Uszkoreit, J.; Jones, L.; Gomez, A.N.; Kaiser, Ł.; Polosukhin, I. Attention is all you need. In Proceedings of the Adv. Neural Inform. Process. Syst., 2017, pp. 5998–6008.
102. Gao, L.; Gopalakrishnan, G.; Nasri, A.; Li, Y.; Zhang, Y.; Ou, X.; Xia, K. Transformer-GCN Fusion Framework for Mineral Prospectivity Mapping: A Geospatial Deep Learning Approach. *Minerals* **2025**, *15*, 711. https://doi.org/10.3390/min15070711.
103. Sabbaghi, H.; Tabatabaei, S.H.; Fathianpour, N. Geologically-constrained GANomaly network for mineral prospectivity mapping through frequency domain training data. *Scientific Reports* **2024**, *14*, 6236. https://doi.org/10.1038/s41598-024-56644-8.
104. Akcay, S.; Atapour-Abarghouei, A.; Breckon, T.P. GANomaly: Semi-supervised anomaly detection via adversarial training. In Proceedings of the Asian Conference on Computer Vision (ACCV). Springer, 2019, pp. 622–637. https://doi.org/10.1007/978-3-030-20893-6_39.
105. Zuo, R.; Luo, Z.; Xiong, Y.; Yin, B. A Geologically Constrained Variational Autoencoder for Mineral Prospectivity Mapping. *Natural Resources Research* **2022**, *31*, 1121–1133. https://doi.org/10.1007/s11053-022-10050-x.
106. Miao, Q.; Wang, P.; Zhao, H.; Li, Z.; Qi, Y.; Mao, J.; Li, M.; Tang, G. Mineral Prospectivity Prediction Based on Self-Supervised Contrastive Learning and Geochemical Data. *Natural Resources Research* **2024**. https://doi.org/10.1007/s11053-024-10335-3.
107. Grill, J.B.; Strub, F.; Altché, F.; Tallec, C.; Richemond, P.H.; Buchatskaya, E.; Doersch, C.; Pinto, B.A.; Zheng, Z.; Azabou, M.; et al. Bootstrap your own latent – a new approach to self-supervised learning. In Proceedings of the Advances in Neural Information Processing Systems (NeurIPS), 2020, Vol. 33, pp. 21271–21284.
108. Meng, Z.; Zuo, R. Self-Supervised Graph Contrastive Learning for Mineral Prospectivity Mapping. *Mathematical Geosciences* **2025**, *57*, 1265–1282. https://doi.org/10.1007/s11004-025-10191-8.
109. Chen, Y.; Chen, B.; Shaylan, A. Semi-supervised graph convolutional networks for integrating continuous and binary evidential layers for mineral exploration targeting. *Ore Geology Reviews* **2024**.
110. Li, Q.; Chen, G.; Wang, D. Mineral Prospectivity Mapping Using Semi-supervised Machine Learning. *Mathematical Geosciences* **2025**, *57*, 275–305. https://doi.org/10.1007/s11004-024-10161-6.
111. Yang, N.; Zhang, Z.; Yang, J.; Hong, Z. Mineral Prospectivity Prediction by Integration of Convolutional Autoencoder Network and Random Forest. *Natural Resources Research* **2022**, *31*, 1103–1119. https://doi.org/10.1007/s11053-022-10038-7.
112. Liu, Y.; Zhang, D.; Li, Z.; Fan, H.; Peng, W. Dirichlet-Based Uncertainty-Aware Deep Learning for Explainable Mineral Prospectivity Mapping. *Natural Resources Research* **2025**. https://doi.org/10.1007/s11053-025-10604-9.
113. Zuo, R.; Cheng, Q.; Xu, Y.; Yang, F.; Xiong, Y.; Wang, Z.; Kreuzer, O.P. Explainable artificial intelligence models for mineral prospectivity mapping. *Science China Earth Sciences* **2024**, *67*, 2864–2875. https://doi.org/10.1007/s11430-024-1309-9.
114. Selvaraju, R.R.; Cogswell, M.; Das, A.; Vedantam, R.; Parikh, D.; Batra, D. Grad-CAM: Visual explanations from deep networks via gradient-based localization. In Proceedings of the IEEE International Conference on Computer Vision (ICCV), 2017, pp. 618–626. https://doi.org/10.1109/ICCV.2017.74.
115. Zhang, Z.J.; Yang, Z.X.; Jian, F.Y.; Ban, S.Y.; Wang, Y.M. Interpretability-Enhanced Mineral Prospectivity Models: A Synergistic Approach Using Large Language Models, Knowledge Graphs, and Machine Learning. *Mathematical Geosciences* **2026**, *58*, 195–231. https://doi.org/10.1007/s11004-025-10231-3.
116. Yin, S.; Li, N.; Xiao, K.; Song, X.; Wang, X. A Dual-Channel Iterative Method Integrating Semi-supervised Self-Training and Interpretable Deep Learning Models for Mineral Prospectivity Prediction. *Natural Resources Research* **2025**, *34*, 2953+. https://doi.org/10.1007/s11053-025-10538-2.
117. Luo, Z.; Farahbakhsh, E.; Hore, S.; Muller, R.D. An explainable semi-supervised deep learning framework for mineral prospectivity mapping: DEEP-SEAM v1.0. *EGUsphere (preprint)* **2025**. https://doi.org/10.5194/egusphere-2025-3283.
118. Shi, Z.; Zuo, R.; Zhou, B. Deep Reinforcement Learning for Mineral Prospectivity Mapping. *Mathematical Geosciences* **2023**, *55*, 773–797. https://doi.org/10.1007/s11004-023-10059-9.

 doi:10.20944/preprints202607.2303.v1

119. Lin, Q.; Zuo, R. Domain Adversarial Neural Network for Mapping Mineral Prospectivity. *Mathematical Geosciences* **2025**, *57*, 471–498. https://doi.org/10.1007/s11004-024-10164-3.
120. Zhang, Z.; Chen, W.; Carranza, E.J.M.; Han, W.; Liu, X.; Li, Y.; Zhang, J.; Li, F.; Lu, Z.; Su, Y.; et al. Deep Subdomain Adaptation Network for Three-Dimensional Mineral Prospectivity Modeling with Imbalanced Data. *Natural Resources Research* **2026**, *35*, 227+. https://doi.org/10.1007/s11053-025-10544-4.
121. Daruna, A.; Zadorozhnyy, V.; Lukoczki, G.; Chiu, H.P. GFM4MPM: Towards Geospatial Foundation Models for Mineral Prospectivity Mapping. *arXiv preprint arXiv:2406.12756* **2024**.
122. Xie, M.; Liu, B.; Li, C.; Li, Y. Geo CNN-Trans: A Hybrid Deep Learning Framework for 3D Mineral Prospectivity Modeling. *Natural Resources Research* **2025**. https://doi.org/10.1007/s11053-025-10612-9.
123. Zhang, Z.; Wang, G.; Carranza, E.J.M.; Du, J.; Li, Y.; Liu, X.; Su, Y. An Uncertainty-Quantification Machine Learning Framework for Data-Driven Three-Dimensional Mineral Prospectivity Mapping. *Natural Resources Research* **2024**, *33*, 1393–1411. https://doi.org/10.1007/s11053-024-10349-x.
124. Prado, E.M.G.; de Souza Filho, C.R.; Carranza, E.J.M.; Motta, J.G. Modeling of Cu-Au prospectivity in the Carajás mineral province (Brazil) through machine learning: Dealing with imbalanced training data. *Ore Geology Reviews* **2020**. https://doi.org/10.1016/j.oregeorev.2020.103611.
125. Parsa, M.; Cumani, R.; Fam, H.J.A.; Tawbe, B. Large Language Models and Geoscience Transformers for Predictive Mapping of Canadian Critical Minerals. *Natural Resources Research* **2026**, *35*, 207+. https://doi.org/10.1007/s11053-025-10564-0.
126. Huang, Y.; Gao, T.; Xu, H.; Zhao, Q.; Song, Y.; Gui, Z.; Lv, T.; Chen, H.; Cui, L.; Li, S.; et al. PEACE: Empowering Geologic Map Holistic Understanding with MLLMs. https://github.com/microsoft/PEACE, 2024.
127. Xiong, Z.; Wang, Y.; Zhang, F.; Stewart, A.J.; Hanna, J.; Borth, D.; Papoutsis, I.; Saux, B.L.; Camps-Valls, G.; Zhu, X.X. Neural plasticity-inspired multimodal foundation model for earth observation. *arXiv preprint arXiv:2403.15356* **2024**.
128. Jakubik, J.; Yang, F.; Blumenstiel, B.; Scheurer, E.; Sedona, R.; Maurogiovanni, S.; Bosmans, J.; Dionelis, N.; Marsocci, V.; Kopp, N.; et al. TerraMind: Large-Scale Generative Multimodality for Earth Observation. *arXiv preprint arXiv:2504.11171* **2025**.
129. Hong, D.; Zhang, B.; Li, X.; Li, Y.; Li, C.; Yao, J.; Yokoya, N.; Li, H.; Ghamisi, P.; Jia, X.; et al. SpectralGPT: Spectral Remote Sensing Foundation Model. *IEEE Transactions on Pattern Analysis and Machine Intelligence* **2024**. https://doi.org/10.1109/TPAMI.2024.3362475.
130. Guo, X.; Lao, J.; Dang, B.; Zhang, Y.; Yu, L.; Ru, L.; Zhong, L.; Huang, Z.; Wu, K.; Hu, D.; et al. SkySense: A Multi-Modal Remote Sensing Foundation Model Towards Universal Interpretation for Earth Observation Imagery. In Proceedings of the Proceedings of the IEEE/CVF Conference on Computer Vision and Pattern Recognition (CVPR), 2024.
131. Danish, M.S.; Munir, M.A.; Shah, S.R.A.; Khan, M.H.; Anwer, R.M.; Laaksonen, J.; Khan, F.S.; Khan, S. TerraFM: A Scalable Foundation Model for Unified Multisensor Earth Observation. *arXiv preprint arXiv:2506.06281* **2025**.
132. Reed, C.J.; Gupta, R.; Li, S.; Brockman, S.; Funk, C.; Clipp, B.; Keutzer, K.; Candido, S.; Uyttendaele, M.; Darrell, T. Scale-MAE: A Scale-Aware Masked Autoencoder for Multiscale Geospatial Representation Learning. In Proceedings of the Int. Conf. Comput. Vis., 2023.
133. Noman, M.; Naseer, M.; Cholakkal, H.; Anwar, R.M.; Khan, S.; Khan, F.S. Rethinking Transformers Pre-training for Multi-Spectral Satellite Imagery. https://github.com/techmn/satmae_pp, 2024.
134. Guo, Z.; Wu, X.; Liang, L.; Sheng, H.; Chen, N.; Bi, Z. Cross-Domain Foundation Model Adaptation: Pioneering Computer Vision Models for Geophysical Data Analysis. *Journal of Geophysical Research: Machine Learning and Computation* **2025**, *2*, e2025JH000601. https://doi.org/10.1029/2025JH000601.
135. Fu, Y.; Wang, M.; Wang, C.; Dong, S.; Chen, J.; Wang, J.; Yu, H.; Huang, J.; Chang, L.; Wang, B. GeoMinLM: A Large Language Model in Geology and Mineral Survey in Yunnan Province. *Ore Geology Reviews* **2025**.
136. NN-Tech. MetalGPT: A Domain-Specific Large Language Model for Mining and Metallurgy. https://huggingface.co/nn-tech/MetalGPT-1, 2025.
137. Massey, M.; Imran, A.A.Z. EarthScape: A Multimodal Dataset for Surficial Geologic Mapping and Earth Surface Analysis. *arXiv preprint arXiv:2503.15625* **2025**.
138. Klemmer, K.; Rolf, E.; Robinson, C.; Mackey, L.; Russwurm, M. SatCLIP: Global, General-Purpose Location Embeddings with Satellite Imagery. In Proceedings of the Proceedings of the AAAI Conference on Artificial Intelligence, 2025, Vol. 39, pp. 4347–4355. https://doi.org/10.1609/aaai.v39i4.32457.

139. Feng, P.; Lv, Z.; Ye, J.; Wang, X.; Huo, X.; Yu, J.; Xu, W.; Zhang, W.; Bai, L.; He, C.; et al. Earth-Agent: Unlocking the Full Landscape of Earth Observation with Agents. In Proceedings of the International Conference on Learning Representations (ICLR), 2026.
140. Shabbir, A.; Sheikh, M.U.; Munir, M.A.; Debary, H.; Fiaz, M.; Zaheer, M.Z.; Fraccaro, P.; Khan, F.S.; Khan, M.H.; Zhu, X.X.; et al. OpenEarthAgent: A Unified Framework for Tool-Augmented Geospatial Agents. *arXiv preprint arXiv:2602.17665* **2026**.
141. He, K.; Chen, X.; Xie, S.; Li, Y.; Dollár, P.; Girshick, R. Masked Autoencoders Are Scalable Vision Learners. In Proceedings of the Proceedings of the IEEE/CVF Conference on Computer Vision and Pattern Recognition (CVPR), 2022, pp. 16000–16009.
142. Claverie, M.; Ju, J.; Masek, J.G.; Dungan, J.L.; Vermote, E.F.; Roger, J.C.; Skakun, S.V.; Justice, C. The Harmonized Landsat and Sentinel-2 surface reflectance data set. *Remote Sensing of Environment* **2018**, *219*, 145–161. https://doi.org/10.1016/j.rse.2018.09.002.
143. Dosovitskiy, A.; Beyer, L.; Kolesnikov, A.; Weissenborn, D.; Zhai, X.; Unterthiner, T.; Dehghani, M.; Minderer, M.; Heigold, G.; Gelly, S.; et al. An Image is Worth 16x16 Words: Transformers for Image Recognition at Scale. In Proceedings of the International Conference on Learning Representations (ICLR), 2021.
144. IBM Research. terratorch: A Fine-Tuning Framework for Geospatial Foundation Models. https://github.com/IBM/terratorch, 2024.
145. Taylor, R.; Kardas, M.; Cucurull, G.; Scialom, T.; Hartshorn, A.; Saravia, E.; Poulton, A.; Kerkez, V.; Stojnic, R. Galactica: A Large Language Model for Science. *arXiv preprint arXiv:2211.09085* **2022**.
146. Mikolov, T.; Chen, K.; Corrado, G.; Dean, J. Efficient Estimation of Word Representations in Vector Space. *arXiv preprint arXiv:1301.3781* **2013**.
147. Pennington, J.; Socher, R.; Manning, C.D. GloVe: Global Vectors for Word Representation. In Proceedings of the Proceedings of the 2014 Conference on Empirical Methods in Natural Language Processing (EMNLP), 2014, pp. 1532–1543. https://doi.org/10.3115/v1/D14-1162.
148. Fuentes, I.; et al. GeoVectoLitho: 3D Models interpolation from word embeddings. https://github.com/IFuentesSR/GeoVectoLitho, 2021.
149. Linphrachaya, N.; Gómez-Méndez, I.; Siripatana, A. Geological Inference from Textual Data using Word Embeddings. *arXiv preprint arXiv:2504.07490* **2025**.
150. Lawley, C.J.; Raimondo, S.; Chen, T.; Brin, L.; Zakharov, A.; Kur, D.; Hui, J.; Newton, G.; Burgoyne, S.L.; Marquis, G. Geoscience language models and their intrinsic evaluation. *Applied Computing and Geosciences* **2022**. https://doi.org/10.1016/j.acags.2022.100084.
151. Huang, Z.; Xu, W.; Yu, K. Bidirectional LSTM-CRF Models for Sequence Tagging. *arXiv preprint arXiv:1508.01991* **2015**.
152. OzRock Contributors. OzRock: A labeled dataset for entity recognition in geological (mineral exploration) domain. https://github.com/majiga/OzROCK, 2023.
153. Hogan, A.; Blomqvist, E.; Cochez, M.; d'Amato, C.; de Melo, G.; Gutierrez, C.; Kirrane, S.; Gayo, J.E.L.; Navigli, R.; Neumaier, S.; et al. Knowledge Graphs. *ACM Computing Surveys* **2021**, *54*, 1–37. https://doi.org/10.1145/3447772.
154. Wang, B.; Wu, L.; Xie, Z.; Qiu, Q.; Zhou, Y.; Ma, K.; Tao, L. Understanding geological reports based on knowledge graphs using a deep learning approach. *Computers & Geosciences* **2022**, *168*, 105229. https://doi.org/10.1016/j.cageo.2022.105229.
155. Liu, Y.; Ott, M.; Goyal, N.; Du, J.; Joshi, M.; Chen, D.; Levy, O.; Lewis, M.; Zettlemoyer, L.; Stoyanov, V. RoBERTa: A Robustly Optimized BERT Pretraining Approach. *arXiv preprint arXiv:1907.11692* **2019**.
156. Graves, A.; Schmidhuber, J. Framewise phoneme classification with bidirectional LSTM and other neural network architectures. *Neural Networks* **2005**, *18*, 602–610.
157. Ma, X. Knowledge graph construction and application in geosciences: A review. *Computers & Geosciences* **2022**, *161*, 105082. https://doi.org/https://doi.org/10.1016/j.cageo.2022.105082.
158. Yang, A.; Yang, B.; Hui, B.; Zheng, B.; Yu, B.; Zhou, C.; et al. Qwen2 Technical Report. *arXiv preprint arXiv:2407.10671* **2024**.
159. Devlin, J.; Chang, M.W.; Lee, K.; Toutanova, K. Bert: Pre-training of deep bidirectional transformers for language understanding. In Proceedings of the Proceedings of the 2019 conference of the North American chapter of the association for computational linguistics: human language technologies, volume 1 (long and short papers), 2019, pp. 4171–4186.
160. Hurst, A.; Lerer, A.; Goucher, A.P.; Perelman, A.; Ramesh, A.; Clark, A.; Ostrow, A.; Welihinda, A.; Hayes, A.; Radford, A.; et al. Gpt-4o system card. *arXiv preprint arXiv:2410.21276* **2024**.

 doi:10.20944/preprints202607.2303.v1

161. Yao, S.; Zhao, J.; Yu, D.; Du, N.; Shafran, I.; Narasimhan, K.; Cao, Y. React: Synergizing reasoning and acting in language models. *arXiv preprint arXiv:2210.03629* **2022**.
162. Yang, A.; Li, A.; Yang, B.; Zhang, B.; Hui, B.; Zheng, B.; Yu, B.; Gao, C.; Huang, C.; Lv, C.; et al. Qwen3 technical report. *arXiv preprint arXiv:2505.09388* **2025**.
163. Hartmann, J.; Moosdorf, N. The new global lithological map database GLiM: A representation of rock properties at the Earth surface. *Geochemistry, Geophysics, Geosystems* **2012**, *13*, Q12004. https://doi.org/10.1029/2012GC004370.
164. Lesur, V.; Hamoudi, M.; Choi, Y.; Dyment, J.; Thébault, E. Building the second version of the World Digital Magnetic Anomaly Map (WDMAM). *Earth, Planets and Space* **2016**, *68*, 27. https://doi.org/10.1186/s40623-016-0404-6.
165. Laske, G.; Masters, G.; Ma, Z.; Pasyanos, M. Update on CRUST1.0 – A 1-degree Global Model of Earth's Crust. In Proceedings of the Geophysical Research Abstracts. European Geosciences Union, 2013, Vol. 15, pp. EGU2013–2658.
166. EarthChem. EarthChem: Community-Driven Preservation and Discovery of Geochemical Data. https://www.earthchem.org/, 2024.
167. Mindat.org. OpenMindat: Open Access to Mineral Data via API. https://www.mindat.org/openmindat, 2024.
168. Wang, Y.; Braham, N.A.A.; Xiong, Z.; Liu, C.; Albrecht, C.M.; Zhu, X.X. SSL4EO-S12: A large-scale multimodal, multitemporal dataset for self-supervised learning in Earth observation [Software and Data Sets]. *IEEE Geoscience and Remote Sensing Magazine* **2023**, *11*, 98–106. https://doi.org/10.1109/MGRS.2023.3281651.
169. Wang, S.; Wang, X.; Deng, F.; Jiang, P.; Chen, J.; Fiandaca, G. OpenEM: Large-scale multi-structural 3D datasets for electromagnetic methods. Data at https://zenodo.org/records/17141981, 2025.
170. Goldman, M.A.; Lederer, G.W.; Rosera, J.M.; Graham, G.E.; Mishra, A.; Yepremyan, A. Extracting data from maps: Lessons learned from the artificial intelligence for critical mineral assessment competition. *Applied Computing and Geosciences* **2025**, *27*, 100274. https://github.com/DARPA-CRITICALMAAS, https://doi.org/10.1016/j.acags.2025.100274.
171. Ley-Cooper, A.Y.; Brodie, R.C.; Richardson, M. AusAEM: Australia's airborne electromagnetic continental-scale acquisition program. *Exploration Geophysics* **2020**, *51*, 193–202, [https://doi.org/10.1080/08123985.2019.1694393]. https://doi.org/10.1080/08123985.2019.1694393.
172. Kirkby, A.L.; Musgrave, R.J.; Czarnota, K.; Doublier, M.P.; Duan, J.; Cayley, R.A.; Kyi, D. Lithospheric architecture of a Phanerozoic orogen from magnetotellurics: AusLAMP in the Tasmanides, southeast Australia. *Tectonophysics* **2020**, *793*, 228560. https://doi.org/https://doi.org/10.1016/j.tecto.2020.228560.
173. Serviço Geológico do Brasil (SGB/CPRM). GeoSGB: Geoscience Data Portal of the Geological Survey of Brazil. https://geosgb.sgb.gov.br/, 2024.
174. Bureau de Recherches Géologiques et Minières (BRGM). Infoterre: BRGM Geological Data Portal. https://infoterre.brgm.fr/, 2024.
175. EIS Horizon EU Project. EIS Toolkit: Python Library for Mineral Prospectivity Mapping. https://github.com/GispoCoding/eis_toolkit, 2023.
176. Raatikainen, M.; Sarala, P.; Ranta, J.P. Self-organizing map modelling and prospectivity mapping of surface geochemical data in Au and multi-metal mineral exploration: example from northern Finland. *Geochemistry: Exploration, Environment, Analysis* **2025**, *25*. https://doi.org/10.1144/geochem2024-055.
177. GemPy Authors. GemPy: Open-source stochastic geological modeling and inversion. https://github.com/cgre-aachen/gempy, 2019.
178. Grose, L.; Ailleres, L.; Laurent, G.; Jessell, M. LoopStructural 1.0: time-aware geological modelling. *Geoscientific Model Development* **2021**, *14*, 3915–3937. https://doi.org/10.5194/gmd-14-3915-2021.
179. Jessell, M.; Ogarko, V.; de Rose, Y.; Lindsay, M.; Joshi, R.; Piechocka, A.; Grose, L.; de la Varga, M.; Ailleres, L.; Pirot, G. Automated geological map deconstruction for 3D model construction using map2loop 1.0 and map2model 1.0. *Geoscientific Model Development* **2021**, *14*, 5063–5092. https://doi.org/10.5194/gmd-14-5063-2021.
180. Uieda, L.; Soler, S.R.; Pesce, A.; Gudknecht, L.J.; et al. Fatiando a Terra: Open-source tools for geophysics. https://github.com/fatiando, 2024. Open-source Python library for geophysics.
181. Rücker, C.; Günther, T.; Wagner, F.M. pyGIMLi: An open-source library for modelling and inversion in geophysics. *Computers & Geosciences* **2017**, *109*, 106–123. https://doi.org/10.1016/j.cageo.2017.07.011.

182. Ogarko, V.; Frankcombe, K.; Liu, T.; Giraud, J.; Martin, R.; Jessell, M. Tomofast-x 2.0: an open-source parallel code for inversion of potential field data with topography using wavelet compression. *Geoscientific Model Development* **2024**, *17*, 2325–2345. https://doi.org/10.5194/gmd-17-2325-2024.
183. Joshi, R.; Madaiah, K.; Jessell, M.; Lindsay, M.; Pirot, G. dh2loop 1.0: an open-source Python library for automated processing and classification of geological logs. *Geoscientific Model Development* **2021**, *14*, 6711–6740. https://doi.org/10.5194/gmd-14-6711-2021.
184. Ogarko, V.; Jessell, M. Automated stratigraphic interpretation from drillhole lithological descriptions with uncertainty quantification: litho2strat 1.0. *Geoscientific Model Development* **2026**, *19*, 1007–1025. https://doi.org/10.5194/gmd-19-1007-2026.
185. Hoyer, S.; Hamman, J. xarray: N-D labeled Arrays and Datasets in Python. *Journal of Open Research Software* **2017**, *5*, 10. https://doi.org/10.5334/jors.148.
186. Corteva Agriscience. rioxarray: geospatial xarray extension powered by rasterio. https://github.com/corteva/rioxarray, 2024.
187. Moore, J.; Kunis, S. Zarr: A Cloud-Optimized Storage for Interactive Access of Large Arrays. In Proceedings of the Proceedings of the Conference on Research Data Infrastructure (CoRDI), 2023. https://doi.org/10.52825/cordi.v1i.285.
188. McGaughey, J.; Brossoit, J.; Davis, K.; Fournier, D.; Hensgen, S. A Framework for Mineral Geoscience Data and Model Portability. *First Break* **2024**, *42*, 89–93. https://doi.org/10.3997/1365-2397.fb2024019.
189. PySpatialML Contributors. PySpatialML: Raster Machine Learning Library. https://github.com/stevenpawley/Pyspatialml, 2022.
190. Chen, K.; Liu, E.; Deng, M.; Tan, X.; Wang, J.; Shi, Y.; Wang, Z. DKNN: deep kriging neural network for interpretable geospatial interpolation. *International Journal of Geographical Information Science* **2024**. https://doi.org/10.1080/13658816.2024.2347316.
191. QGIS Development Team. QGIS: A Free and Open Source Geographic Information System. https://qgis.org/, 2024.
192. PyVista Contributors. PyVista: 3D plotting and mesh analysis through a streamlined interface for VTK. https://github.com/pyvista/pyvista, 2019.
193. Microsoft Research. InterpretML: Interpreting models of tabular data. https://github.com/interpretml/interpret, 2019.
194. Lundberg, S.M.; Lee, S.I. A Unified Approach to Interpreting Model Predictions. In Proceedings of the Adv. Neural Inform. Process. Syst., 2017.
195. Zuo, R.; Wang, Z. Effects of Random Negative Training Samples on Mineral Prospectivity Mapping. *Natural Resources Research* **2020**, *29*, 3443–3455. https://doi.org/10.1007/s11053-020-09668-6.
196. Garcia, L.F.; Abel, M.; Perrin, M.; Alvarenga, R.d.S. The GeoCore ontology: A core ontology for general use in Geology. *Computers & Geosciences* **2020**, *135*, 104387. https://doi.org/10.1016/j.cageo.2019.104387.
197. Kendall, A.; Gal, Y. What Uncertainties Do We Need in Bayesian Deep Learning for Computer Vision? In Proceedings of the Adv. Neural Inform. Process. Syst., 2017, Vol. 30.
198. Jospin, L.V.; Laga, H.; Boussaid, F.; Buntine, W.; Bennamoun, M. Hands-on Bayesian neural networks—A tutorial for deep learning users. *IEEE Computational Intelligence Magazine* **2022**, *17*, 29–48.
199. Gal, Y.; Ghahramani, Z. Dropout as a Bayesian Approximation: Representing Model Uncertainty in Deep Learning. In Proceedings of the Proceedings of The 33rd International Conference on Machine Learning, 2016, Vol. 48, *PMLR*, pp. 1050–1059.
200. Shafer, G.; Vovk, V. A Tutorial on Conformal Prediction. *Journal of Machine Learning Research* **2008**, *9*, 371–421.
201. Zhang, Z.; Wang, G.; Liu, C.; Cheng, L.; Sha, D. Bagging-based positive-unlabeled learning algorithm with Bayesian hyperparameter optimization for three-dimensional mineral potential mapping. *Computers & Geosciences* **2021**, *154*, 104817. https://doi.org/https://doi.org/10.1016/j.cageo.2021.104817.
202. Chawla, N.V.; Bowyer, K.W.; Hall, L.O.; Kegelmeyer, W.P. SMOTE: Synthetic Minority Over-sampling Technique. *Journal of Artificial Intelligence Research* **2002**, *16*, 321–357. https://doi.org/10.1613/jair.953.
203. Settles, B. Active Learning Literature Survey. Computer Sciences Technical Report 1648, University of Wisconsin–Madison, 2009.

 doi:10.20944/preprints202607.2303.v1

204. Haan, S.; Ramos, F.; Müller, R.D. Multiobjective Bayesian optimization and joint inversion for active sensor fusion. *Geophysics* **2021**, *86*, ID1–ID17. https://doi.org/10.1190/geo2019-0460.1.
205. Thiele, S.T.; Jessell, M.W.; Lindsay, M.; Ogarko, V.; Wellmann, J.F.; Pakyuz-Charrier, E. The topology of geology 1: Topological analysis. *Journal of Structural Geology* **2016**, *91*, 27–38. https://doi.org/https://doi.org/10.1016/j.jsg.2016.08.009.